Vol. 637: 117–140, 2020
https://doi.org/10.3354/meps13211

MARINE ECOLOGY PROGRESS SERIES
Mar Ecol Prog Ser

Published March 5

Spatial and temporal dynamics of Pacific capelin *Mallotus catervarius* in the Gulf of Alaska: implications for ecosystem-based fisheries management

David W. McGowan[1,7,*], Esther D. Goldstein[2], Mayumi L. Arimitsu[3], Alison L. Deary[2], Olav Ormseth[2], Alex De Robertis[2], John K. Horne[1], Lauren A. Rogers[2], Matthew T. Wilson[2], Kenneth O. Coyle[4], Kristine Holderied[5], John F. Piatt[6], William T. Stockhausen[2], Stephani Zador[2]

[1]School of Aquatic and Fishery Sciences, University of Washington, Seattle, WA 98195, USA
[2]Alaska Fisheries Science Center, National Marine Fisheries Service (NMFS), National Oceanic and Atmospheric Administration (NOAA), Seattle, WA 98115, USA
[3]US Geological Survey, Alaska Science Center, 250 Egan Dr., Juneau, AK 99801, USA
[4]Institute of Marine Science, University of Alaska, Fairbanks, AK 99775-7220, USA
[5]NOAA National Ocean Service, National Centers for Coastal Ocean Science, Kasitsna Bay Laboratory, 95 Sterling Highway, Suite 2, Homer, AK 99603, USA
[6]US Geological Survey, Alaska Science Center, 4210 University Dr., Anchorage, AK 99508, USA
[7]*Present address:* Alaska Fisheries Science Center, National Marine Fisheries Service (NMFS), National Ocean and Atmospheric Administration (NOAA), Seattle, WA 98115, USA

ABSTRACT: Pacific capelin *Mallotus catervarius* are planktivorous small pelagic fish that serve an intermediate trophic role in marine food webs. Due to the lack of a directed fishery or monitoring of capelin in the Northeast Pacific, limited information is available on their distribution and abundance, and how spatio-temporal fluctuations in capelin density affect their availability as prey. To provide information on life history, spatial patterns, and population dynamics of capelin in the Gulf of Alaska (GOA), we modeled distributions of spawning habitat and larval dispersal, and synthesized spatially indexed data from multiple independent sources from 1996 to 2016. Potential capelin spawning areas were broadly distributed across the GOA. Models of larval drift show the GOA's advective circulation patterns disperse capelin larvae over the continental shelf and upper slope, indicating potential connections between spawning areas and observed offshore distributions that are influenced by the location and timing of spawning. Spatial overlap in composite distributions of larval and age-1+ fish was used to identify core areas where capelin consistently occur and concentrate. Capelin primarily occupy shelf waters near the Kodiak Archipelago, and are patchily distributed across the GOA shelf and inshore waters. Interannual variations in abundance along with spatio-temporal differences in density indicate that the availability of capelin to predators and monitoring surveys is highly variable in the GOA. We demonstrate that the limitations of individual data series can be compensated for by integrating multiple data sources to monitor fluctuations in distributions and abundance trends of an ecologically important species across a large marine ecosystem.

KEY WORDS: Population dynamics · Connectivity · Spawning habitat · Individual-based model · Larval drift · Small pelagic fish · Forage fish

1. INTRODUCTION

Small pelagic fishes serve an intermediate trophic role as consumers of zooplankton and prey for marine predators. Piscivorous seabirds, marine mammals, and fishes are affected by changes in the availability of planktivorous fishes (Cury et al. 2000), and ecosystem-based fisheries management is increasingly con-

*Corresponding author: david.mcgowan@noaa.gov

sidering populations of ecologically important forage species that are not commercially exploited (Link 2002, Pikitch et al. 2004, Francis et al. 2007). Detecting temporal changes in distributions and abundances of small pelagic fishes is difficult due to a lack of directed sampling for these species that is further complicated by their aggregation behavior and variable ontogenetic habitat use that may span large spatial domains. Accordingly, there are limitations associated with using data from surveys designed for commercial species to assess non-targeted species, as the spatial coverage of the survey and sampling gear used may not be appropriate to quantify small pelagic fish occurrence and density. To gain insights on the life history, spatial patterns, and population dynamics of an ecologically important fish species, Pacific capelin *Mallotus catervarius* (=*M. villosus*, see Mecklenburg et al. 2018), this study integrated analyses of modeled spawning habitat and larval dispersal with the synthesis of spatially indexed data from multiple, independent surveys in the Gulf of Alaska (GOA).

Pacific capelin (hereafter capelin) are small pelagic schooling fish found in North Pacific and Arctic waters that extend from the nearshore across the continental shelf and to the upper slope (Mecklenburg & Steinke 2015). Capelin are short-lived and primarily semelparous (i.e. they spawn once and die), with most spawning by age 2 or 3 (Pahlke 1985, M. Arimitsu unpubl. data) in the intertidal zone on gravel beaches and in rivers (Stergiou 1989). Limited observations of capelin spawning indicate that the location and timing of spawning varies across the GOA, primarily occurring from late spring through summer, depending on region (Blackburn et al. 1981, Pahlke 1985, Brown 2002, Arimitsu et al. 2008). Requirements for specific spawning substrates are likely influenced by additional needs for optimal water temperatures (Carscadden et al. 1989, 1997), which may lead to interannual shifts in spawn distributions across the GOA as observed in the Atlantic (e.g. Gjøsæter 1998). After hatching from demersal eggs, the larvae are located near the surface and are transported from the nearshore spawning locations to offshore nursery areas over the shelf by tidal flushing and wind-driven currents (Doyle et al. 2002, Lanksbury et al. 2005). The larval phase lasts for approximately 12 mo before juvenile metamorphosis (Doyle et al. 2019), during which transport pathways for larvae over the shelf are unknown. Immature capelin, ages 1 yr and older (hereafter age-1+), occur in both offshore and inshore waters of the GOA, indicating that an unknown proportion of larvae is retained within inshore embayments (Brown 2002, Arimitsu et al. 2008). Age-1+ capelin are patchily distributed offshore over the shelf (Mueter & Norcross 2002, Piatt et al. 2018, McGowan et al. 2019a,b), as well as in coastal and inshore waters around the Kodiak Archipelago (hereafter Kodiak; Blackburn et al. 1981, Pahlke 1985), lower Cook Inlet (Abookire & Piatt 2005, Speckman et al. 2005), Prince William Sound (Brown 2002), and southeast Alaska (Arimitsu et al. 2008) (see Fig. 1).

Capelin are mobile and gregarious, and spatial and temporal fluctuations in their distributions affect their availability as prey to piscivorous seabirds (Hatch 2013, Sydeman et al. 2017), marine mammals (Witteveen et al. 2008), and commercially important fishes (Aydin et al. 2007). Unlike *M. villosus* populations in the Atlantic, capelin have not been commercially exploited in the Northeast (NE) Pacific, nor have they been a focal species for fisheries abundance surveys. Nearly all studies of capelin in the NE Pacific have been limited by 1 or more of the following factors: temporal duration (typically ≤3 yr); spatial coverage (e.g. study area of ~10s to 100s of km versus the population's range of ~1000s of km); sampling biases associated with fixed-depth gear, trawl selectivity, temporal sampling (e.g. differences in diel catch rates), and/or uncertainties in acoustic identification of capelin; and indirect sampling (e.g. abundance inferred from predator diets). As a result, a comprehensive assessment of capelin life history and population dynamics has not been conducted in the GOA or elsewhere in the NE Pacific, but is needed to evaluate how spatio-temporal changes in their availability as prey impacts managed piscivores under an ecosystem-based approach to fisheries management.

To overcome these methodological challenges and gain insights on an ecologically important forage species, we attempted to compensate for the limitations of individual data series by integrating multiple, independent data sources from groundfish abundance and ecosystem monitoring surveys with spawning habitat and larval dispersal models to explore relatively unstudied processes and synthesize current understanding of spatial patterns and trends in the GOA capelin population over the past 2 decades. The specific objectives of the study were to:

(1) characterize important features of capelin spawning habitat from observational data and identify potential capelin spawning habitat throughout the GOA;

(2) simulate larval dispersal in the GOA to assess connectivity between inshore spawning areas and offshore distributions of larval capelin;

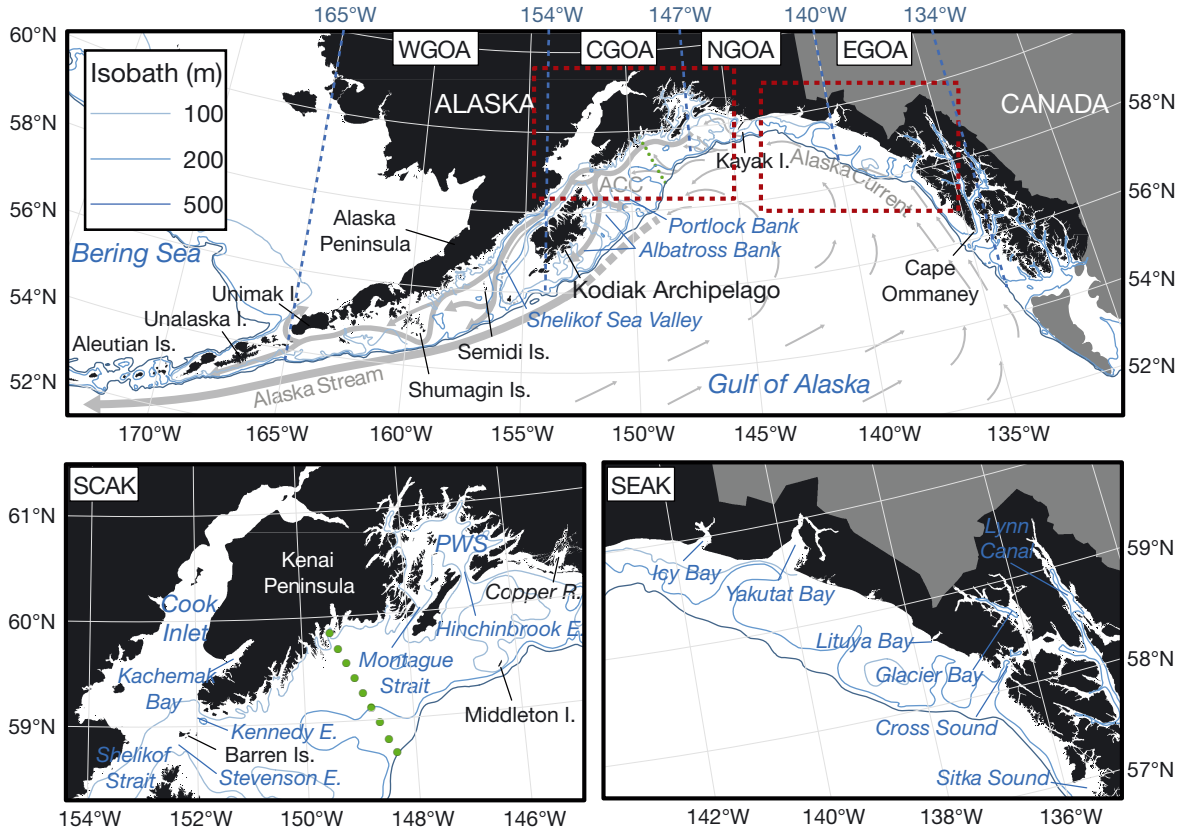

Fig. 1. Gulf of Alaska (GOA) study area. Major circulation features (gray), including the Alaska Current, Alaska Stream, and Alaska Coastal Current (ACC), are adapted from Stabeno et al. (2004, 2016a,b). Key bathymetric (cyan) and geographic (black/white) features mentioned in text are labeled. Longitudinal subdivisions (dotted blue lines) over the continental shelf (<500 m) identify the western (WGOA), central (CGOA), northern (NGOA), and eastern (EGOA) offshore regions. Red boxes in upper map identify the Southcentral Alaska (SCAK) and Southeast Alaska (SEAK) inshore regions. Green dots indicate Seward Line stations; PWS: Prince William Sound

(3) synthesize available survey data to characterize spatial and temporal distributions of capelin in inshore and offshore waters of the GOA;

(4) develop a conceptual model of capelin spatial patterns and connectivity between spawning habitats and high-density observations of larval and age-1+ fish in the GOA.

2. METHODS

2.1. Study area

The GOA ecosystem is characterized by complex topography and circulation. Numerous fjords and coastal embayments line the GOA coastline, while troughs and deep canyons occur on the continental shelf (Mundy 2005, Zimmermann & Prescott 2015, Mordy et al. 2019) (Fig. 1). Two major circulation patterns occur in the GOA (Fig. 1): a cyclonic subarctic gyre around the deep basin, and the Alaska Coastal Current (ACC) over the shelf (Stabeno et al. 2004, 2016a, Ladd et al. 2005). The gyre's eastern boundary current, the Alaska Current, flows northward along the coast of southeast Alaska (Stabeno et al. 2016b). In the northern GOA, the Alaska Current turns southwestward, where it diverges into the Alaskan Stream and the ACC (Stabeno et al. 2004). The Alaskan Stream is a narrow, high-speed western boundary current that runs along the upper slope parallel to the shelf break towards the Aleutian Islands (Stabeno et al. 2004). Over the shelf, the ACC's flow is continuous yet highly variable, driven by alongshore winds and freshwater inputs from rivers (Royer 1982, Stabeno et al. 2004, 2016a).

To account for differences in spatial sampling among data sources used to assess capelin distribution and abundance, the GOA was divided into 2 inshore and 5 offshore regions (Fig. 1). The inshore regions included: southeast Alaska inner waters (SEAK: Glacier Bay, Cross Sound, Sitka Sound, Yakutat Bay, and Icy Bay) and southcentral Alaska (SCAK:

Cook Inlet, coastal embayments along the Kenai Peninsula, and Prince William Sound). Offshore waters deeper than 500 m bottom depth were defined as the 'slope,' while offshore regions over the GOA shelf (<500 m) were defined by longitude: eastern shelf (EGOA: 134–140° W); northern shelf (NGOA: 140–147° W); central shelf (CGOA: 147–154° W); and western shelf (WGOA: 154–165° W).

2.2. Classification of potential spawning habitat

To provide baseline information regarding capelin spawning in the GOA, we combined spawning observations with a comprehensive database of shoreline habitats. Capelin in the North Pacific are believed to only spawn in the intertidal zone along gravel beaches and in rivers (Stergiou 1989), unlike in the Atlantic where capelin *M. villosus* also spawn demersally in offshore waters (Sætre & Gjøsæter 1975, Carscadden et al. 1989). Therefore, we focused our analysis on shoreline habitats and used the ShoreZone Coastal Habitat Mapping System (https://alaskafisheries.noaa.gov/habitat/shorezone-reports), a database that describes coastline habitat throughout the GOA in a consistent manner. ShoreZone assigns geomorphic and biological attributes to alongshore segments based on imagery collected during low-altitude aerial surveys (Harper & Morris 2014). Information compiled from 28 sites where capelin spawning was either directly observed or inferred from the presence of adults in spawning condition (Table S1 in Supplement 1 at www.int-res.com/articles/suppl/m637p117_supp.pdf) was combined with ShoreZone data to define criteria that best described capelin spawning habitats (Fig. 2A). Because many of the identified capelin spawning sites had imprecise geographical coordinates, a 1 km buffer was created around each known point, and all ShoreZone units that fell within that buffer were selected as potential descriptors of spawning habitat. The ShoreZone attribute values for each selected unit were collated to identify common values among sites.

Twelve attributes had values that occurred consistently in multiple units and were chosen for identifying potential spawning habitat (Table 1). Attributes for shore type (*BC_CLASS*) and an environmental sensitivity index (*ESI*) are general descriptors that aggregate multiple characteristics in a single value (e.g. an *ESI* value of 9A indicates sheltered tidal flats). The attribute *EXP_BIO* indicates exposure to wave activity. The remaining 9 attributes describe specific characteristics of 3 intertidal across-shore subcomponents (B_1–B_3; few of the units had >3 subcomponents). For each subcomponent, attributes described primary landform (e.g. beach, cliff), primary substrate (e.g. clastic, bedrock), and the slope angle. We did not further specify particle size or sediment composition using substrate characteristics from other studies (e.g. Nakashima & Taggart 2002) due to uncertainty in the accuracy of aerial survey observations for these metrics in the ShoreZone database. The selection query for the subcomponents was structured so that at least 1 subcomponent had to meet the necessary criteria.

Because the ShoreZone habitat data are highly complex and multiple values were identified for each attribute, we defined 2 levels of habitat classification, permissive and restrictive, based on the cumulative frequency distributions for each attribute. Permissive classification included the combination of values that, when ranked from most common to least common, described at least 75% of the buffer-selected ShoreZone units. The restrictive classification included the ranked values that described less than 75% of the units (Table 1). For example, the permissive *BC_CLASS* criteria (types 24, 28, and 31) were found in 83% of the units, while the restrictive criteria (24 and 31) occurred in 63% of the units.

The 2 sets of criteria were used to query the database of all ShoreZone units in the GOA. The resulting selections, as well as the entire dataset, were aggregated into 40×40 km grid cells encompassing the GOA coast. For each level of classification, an index of potential spawning habitat density was calculated as the sum of selected shoreline lengths (km) divided by the total length of shoreline in each grid cell. Analyses were conducted using GIS (ArcGIS 10.3, ESRI).

2.3. Simulation of larval transport

The influence of ocean circulation and dispersal on larval distributions and connectivity between known capelin spawning locations and distributions of larval capelin over the GOA shelf (see Section 2.4.) were explored using the Dispersal Model for Early Life Stages (DisMELS), an individual-based biophysical modeling (IBM) framework used to examine pelagic larval dispersal for marine organisms in the GOA (Cooper et al. 2013, Duffy-Anderson et al. 2013, Stockhausen et al. 2019). The model coupled coarse capelin early life-history characteristics with daily averaged output from the Regional Ocean Modeling System (ROMS: https://www.myroms.org), a primi-

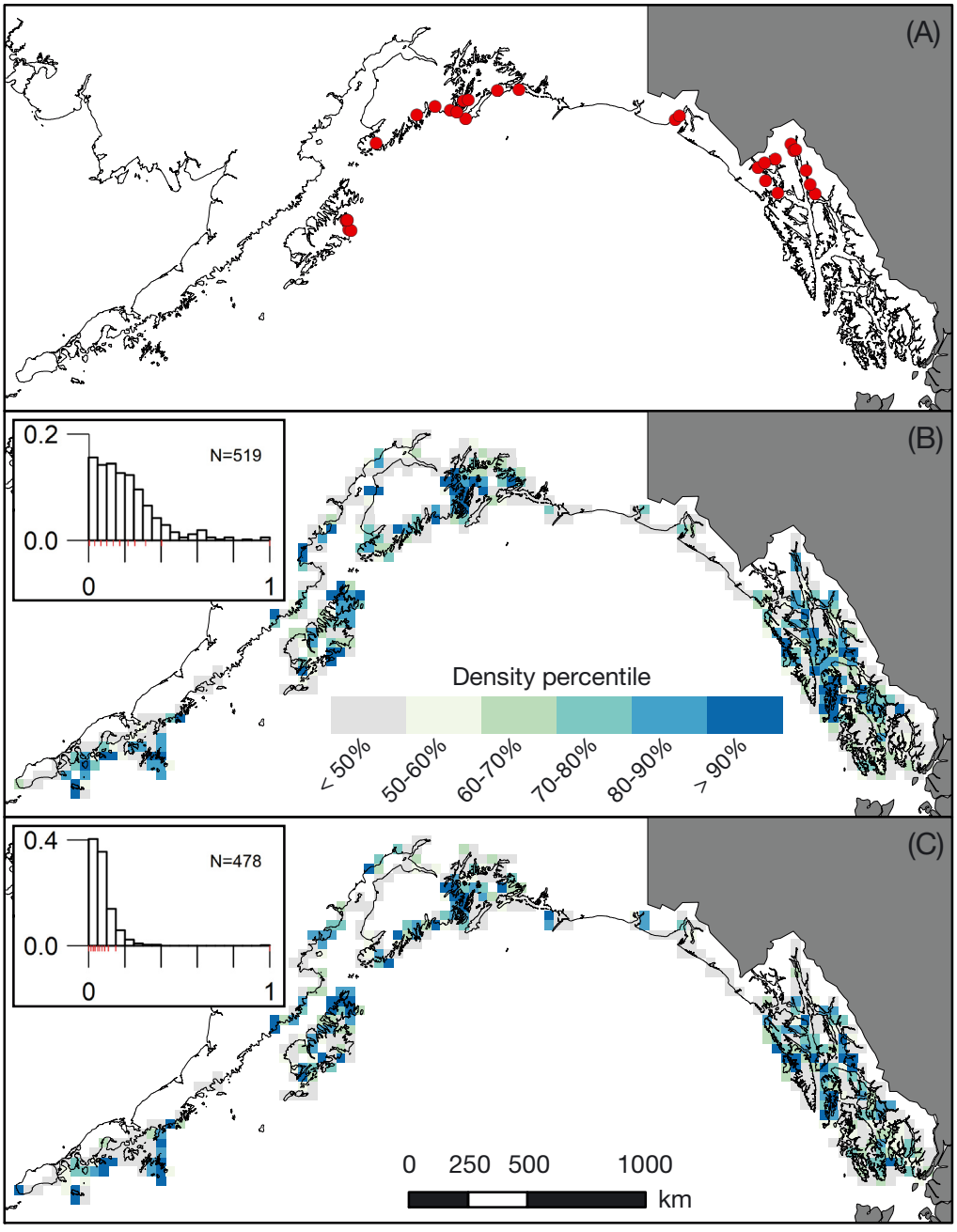

Fig. 2. Observed and predicted capelin spawning in the Gulf of Alaska. (A) Observed or inferred spawning locations (red dots). Density percentiles and density values of predicted capelin spawning habitat based on (B) permissive and (C) restrictive selection criteria (see Table 1). Red ticks in density histograms (insets) indicate 10% quartile intervals. Note that only grid cells with non-zero density values are shown

tive-equation 3-dimensional ocean circulation model driven by atmospheric forcing. The ROMS model incorporated nested models (NPac with 20–40 km resolution, NEP with 10 km resolution, CGOA with 3 km resolution) where coarser grids set boundary conditions for finer-resolution grids (Shchepetkin & McWilliams 2005, Haidvogel et al. 2008, Hermann et al. 2009, Coyle et al. 2013).

Using the DisMELS framework (Table 2; see details in Stockhausen et al. 2019), particles representing capelin larvae were released within the GOA, with model domain extent defined by the 3 km CGOA ROMS grid. Simulated larvae were released from 9 point locations (Fig. S1 in Supplement 2) that were located just offshore of known inshore spawning locations for capelin to minimize any limitation of the

Table 1. ShoreZone coastal habitat mapping attributes used for predicting capelin spawning habitat and the attribute values corresponding to permissive selection criteria. Attributes that correspond to restrictive selection criteria (Res) are indicated by an 'x'. Multiple categorical or numeric values are indicated by an asterisk (*). For further explanation of the attribute values, refer to the ShoreZone website (https://alaskafisheries.noaa.gov/habitat/shorezone-reports)

Attribute	Description	Value	Description	Res
BC_CLASS	Shore type	31	Estuarine processes dominant structuring of shore type	x
		24	Wave-structured; sand & gravel flat or fan (<5°), wide (>30 m)	x
		28	Wave-structured, sand flat (<5°), wide (>30 m)	
ESI	Environmental sensitivity index	5	Mixed sand and gravel beaches (cf. Table 14 in Harper & Morris 2014)	
		9A	Sheltered tidal flats	x
		10A	Salt- and brackish-water marshes	x
EXP_BIO	Biological wave exposure	*	All values selected except exposed (E) and very exposed (VE)	x
Form1_B$_i$	Principal geomorphic feature (i.e. landform) within across-shore component of the intertidal zone[a]	B	All beach features	x
		P	All platform features	
		T	All tidal flat features	
Mat1_B$_i$	Substrate that best characterizes *Form1_B$_i$*	C	All clastic sediments[b]	x
SLOPE_B$_i$	Estimated across-shore slope of *Form1_B$_i$*	*	Average slope within one of the B$_i$ components was < 20°	x

[a]The intertidal zone may be comprised of 1 to 3 components (B_1, B_2, B_3) indexed by i, in which the component with the lower number is located higher on the shore. One of the B_i components must be of a low slope form (e.g. *Form1_B$_1$* can be cliff if *Form1_B$_2$* is beach)

[b]Includes sand, pebbles, rock, cobble, and boulders because we anticipated high uncertainty in the proportional composition of substrate materials based on identification from aerial surveys

ROMS model to resolve nearshore circulation. The model was run for 2 climatically contrasting years: 2003 (an El Niño year), and 2011 (a strong La Niña year) (Multivariate ENSO Index: https://www.esrl.noaa.gov/psd/enso/mei; Wolter & Timlin 1993, 1998). Simulated larvae were released daily from the 10th to the 20th day of May, June, and July of each study year (10 d cohorts), with a model duration from May–November to capture general dispersal patterns from spawning locations. Larvae were assigned a vertical swim speed of 0.003 m s^{-1} to maintain their vertical position within the assigned depth interval (Sohn 2016). Based on historic vertical distribution data from multiple opening/closing net and environmental sensing system (MOCHNESS) samples collected in the CGOA region in 2002 and 2004 (D. Cooper unpublished data), larvae were separated into 2 life stages to correspond to vertical distributions associated with ontogeny (Fig. S2): pre-flexion larvae were assigned a preferred depth of 20–50 m, and post-flexion larvae had a preferred depth of 50–80 m. No other biological characteristics differed between life stages in the model. Transition between pre-flexion and post-flexion larvae occurred at 7 mm length and was based on a growth rate of 0.1 mm d^{-1} following Doyle et al. (2002), a calculated growth estimate at a temperature of ~6°C during the study months (Stabeno et al. 2016a), and an estimated 8 h of bright sunshine (Frank & Leggett 1982). Vertical and horizontal particle diffusion rates were each set at 0.001 m^2 s^{-1} (Sohn 2016) with diffusive particle movement incorporating swimming and horizontal or vertical random walks. Mortality was not included in the model because the goal of this study was to identify potential connectivity pathways and source locations for larvae. Age, size, and developmental stage of simulated larvae were tracked in 20 min time steps with particle locations (latitude, longitude, depth) updated using a fourth-order predictor-corrector algorithm (Stockhausen et al. 2019).

To identify dispersal patterns, potentially important spawn locations, and regions of larval accumulation, model outputs were plotted as heatmaps to depict simulated larval accumulation in each region (Fig. 1) by month for each spawning (i.e. release) location (1–9, Fig. S1). To display daily model output, temporal heatmaps depict the proportion of daily larval observations in each region by month (May–

Table 2. Summary of individual-based biophysical model parameters for each of the life stages simulated in the model. NA: not applicable

Parameter	Pre-flexion	Post-flexion
Daily particle release dates	10–20 May, 2003 and 2011 10–30 June, 2003 and 2011 10–20 July, 2003 and 2011	NA
Preferred depth range (m)	20–50	50–80
Vertical swim speed (m s^{-1})	0.003	0.003
Size at transition to next stage (mm)	7	NA
Growth rate (mm d^{-1})	0.1	0.1
Vertical diffusion rate (m^2 s^{-1})	0.001	0.001
Horizontal diffusion rate (m^2 s^{-1})	0.001	0.001
Time step (min)	20	20
Model output	Daily	Daily

November) compared to the total potential number of larval observations based on the number of virtual larvae spawned:

$$\text{Proportion} = \frac{\sum \text{daily larval count released from location } x \text{ in region } y \text{ during month } z}{\sum \text{daily total potential larval count during month } z} \quad (1)$$

For example, if 10 virtual larvae spawned from location 1 were located in the CGOA region throughout May (31 d), then the numerator would be 10 larvae × 31 d. The denominator is a total cumulative sum based on larvae that were spawned. Therefore, if a total of 90 larvae were spawned prior to 1 May across all 9 spawn locations, then the denominator would be 90 larvae × 31 d. This calculation includes larvae that exited the model domain. Daily model output was also plotted showing dispersal paths for May, June, and July spawning cohorts from each spawn location.

2.4. Characterization of stage-specific distributions

To identify areas of the GOA where capelin consistently occur and concentrate, spatial patterns of capelin catch per unit effort (CPUE) were compared among multiple, independent surveys conducted within inshore and/or offshore waters over the GOA shelf (Table 3). Detailed descriptions of each data source are provided in Tables S2–S7 in Supplement 1. Briefly, capelin CPUEs for larval (<6 cm fork length, L_F) and age-1+ fish (>6 cm L_F) were collected between 1996 and 2016 within inshore waters of the SCAK and SEAK regions by the US Geological Survey (USGS) using beach seines and 2 types of midwater trawls (Table S2; hereafter USGS survey). In offshore waters, capelin CPUEs were collected between 2000 and 2015 during surveys conducted by the National Oceanographic and Atmospheric Administration's Alaska Fisheries Science Center (NOAA-AFSC) designed for either ecosystem monitoring or estimating abundances of walleye pollock *Gadus chalcogrammus* (hereafter pollock) and other groundfish species. Larval capelin CPUEs were collected during ecosystem surveys using ichthyoplankton nets (Table S3; hereafter EC survey). Trawl- and acoustic-based measures of age-1+ capelin CPUEs were collected over the GOA shelf and upper slope during 4 surveys: a small-mesh, midwater trawl survey designed for young-of-the-year pollock (Table S4; hereafter MT survey), a bottom trawl survey designed for groundfish (Table S5; hereafter BT survey), an acoustic-trawl survey designed for age-1+ pollock (Table S6; hereafter AT survey), and an acoustic-trawl survey designed for ecosystem monitoring (Table S7; hereafter GE survey). With the exception of the inshore USGS surveys, capelin was not a focal species during the design or sampling of any surveys. USGS sampling was spatially limited to a subset of inshore locations each year. Data collected before and after the offshore data study period (2000 to 2015) were included to expand this study's spatial coverage and/or increase low sample sizes (Table S2).

Length measurements were plotted as relative frequencies by life stage (standard length, L_S, for larvae; L_F for age-1+) to identify length modes and range of sizes sampled by each survey. Inshore capelin lengths were pooled across years and gear types by life stage (larval, age-1+) and region, while offshore age-1+ lengths were pooled across years by survey. Length measurements (cm) for inshore larvae were converted from total lengths (L_T) to L_S using the relationship between paired measurements (n = 44): $L_S = 0.884 \times L_T + 1.0306$ ($R^2 = 0.997$). Since only a subset of larvae is measured at each station (maximum = 50 ind. $taxon^{-1}$), capelin size composition at each station was calculated using length frequencies to apportion the total catch; size compositions were summed across station by season and expressed as proportions. L_S measurements for age-1+ fish from the MT and AT surveys were converted to L_F using an equation derived from a subset of fresh capelin collected during the AT survey from which all 3 length measurements (cm) were taken (n = 221): $L_F = 1.0563 \times L_S + 0.0364$ ($R^2 = 0.997$).

Table 3. Summary of data sources. Coverage by survey (USGS: inshore survey; EC: ecosystem ichthyoplankton survey; MT: midwater trawl survey; BT: bottom trawl survey; AT: pollock acoustic-trawl survey; GE: ecosystem acoustic-trawl survey), region (see Fig. 1), year, season (Sp: spring; Su: summer; Fa: fall), and sampling gear (60BN: 60 cm bongo net; AWT: Aleutian wing trawl; BS: beach seine; CT: Cantrawl; EK60 and ES60: EK60 and ES60 echosounders, respectively; IKMT: Isaacs-Kidd midwater trawl; MHT: modified herring trawl; PNE: poly Nor'eastern trawl; ST: Stauffer trawl; TT: Tucker trawl)

Survey	Region (location)	Year	Season	Gear
USGS	SCAK (Cook Inlet)	1996–1999, 2016–2017	Su	MHT
	(Kenai Fjords)	2007–2008	Su	BS, IKMT
	(Prince William Sound)	2010, 2012–2016	Su	BS, MHT
	SEAK (Yakutat Bay, Icy Bay)	2002, 2011	Su	BS, MHT
	(Outer Coast, Icy Strait, Skagway)	1999–2003	Su	BS, IKMT, MHT
	(Glacier Bay)	1999–2004	Su	BS, IKMT, MHT
EC	WGOA	2000–2013. 2015	Sp	60BN
		2000, 2003, 2005, 2009–2015[a]	Su	60BN
		2000–2005, 2007, 2009	Fa	TT
		2011, 2013, 2015		60BN
	CGOA	2001–2007, 2010–2011, 2013, 2015	Sp	60BN
		2000–2006, 2009–2013, 2015	Su	60BN
		2000–2005, 2007, 2009	Fa	TT
		2011, 2013		60BN
	NGOA	2003, 2005, 2007, 2011, 2013, 2015	Sp	60BN
		2002, 2004, 2011–2015	Su	60BN
	EGOA	2005, 2010–2011, 2013	Sp	60BN
		2010–2015	Su	60BN
		2014–2015	Fa	60BN
MT	WGOA	2000, 2001–2015[a]	Fa	ST
	CGOA	2005–2015[a]	Fa	ST
BT	WGOA, CGOA, NGOA	2001–2015[a]	Su	PNE
	EGOA	2003–2015[a]	Su	PNE
AT	WGOA, CGOA	2003, 2005, 2011–2015[a]	Su	EK60, AWT
	NGOA	2003, 2013, 2015	Su	EK60, AWT
	EGOA	2013, 2015	Su	EK60, AWT
GE	CGOA, NGOA, EGOA	2011, 2013	Su, Fa	ES60, CT

[a]Odd years only

To facilitate comparisons among the different survey designs and sampling gears, CPUE data were normalized (nCPUE) by the sum of catches within the following strata:

USGS survey:

$$\text{nCPUE} = \frac{\text{CPUE for inshore region } r \text{ and gear type } g}{\sum \text{CPUE for inshore region } r \text{ and gear type } g} \quad (2)$$

EC survey:

$$\text{nCPUE} = \frac{\text{CPUE for year } t \text{ and season } s}{\sum \text{CPUE for year } t \text{ and season } s} \quad (3)$$

MT survey:

$$\text{nCPUE} = \frac{\text{CPUE for year } t \text{ and diel period } d}{\sum \text{CPUE for year } t \text{ and diel period } d} \quad (4)$$

BT and AT surveys:

$$\text{nCPUE} = \frac{\text{CPUE for year } t}{\sum \text{CPUE for year } t} \quad (5)$$

GE survey:

$$\text{nCPUE} = \frac{\text{CPUE for offshore region } y}{\sum \text{CPUE for offshore region } y} \quad (6)$$

This normalization was intended to highlight areas where capelin consistently occur in years of both high and low abundance. USGS survey data were not normalized by year due to low sample sizes within each region–gear stratum (Table S2), and therefore distributions do not account for interannual variability.

Distributions of nCPUEs were mapped by life stage (larval, age-1+) for inshore and offshore surveys. For each inshore region and life stage, nCPUEs from

USGS surveys were averaged across years and gear types within 10 × 10 nautical mile (n mile; 18.5 × 18.5 km) grid cells and plotted as density percentiles in 10% increments. For each offshore survey, nCPUEs for age-1+ fish were averaged across years within 20 × 20 n mile (37 × 37 km) grid cells and similarly plotted as density percentiles, while nCPUEs for larval capelin from the EC survey were averaged across years by season (spring, summer, fall) in 20 × 20 n mile cells.

2.5. Age-1+ distributions relative to bottom depth

Catch rates and vertical distributions of age-1+ capelin were quantified relative to bottom depth over the GOA shelf to assess whether differences in spatial patterns among the 4 offshore surveys were related to sample designs and coverage. For each age-1+ offshore survey, raw CPUEs (kg km^{-2} for BT, MT, and AT surveys; acoustic backscatter attributed to capelin, s_A, m^2 n mile^{-1}, for GE survey) from all years were plotted relative to bottom depth, and the mean bottom depths were calculated for all samples in the survey, samples where capelin were present (CPUE > 0), and for all samples weighted by capelin biomass density. Interannual variability in occurrence frequencies was also examined in 2 bottom depth strata (<100 m = 'shallow,' 100–300 m = 'deep') by survey. Finally, vertical distributions from GE surveys in 2011 and 2013 were characterized following McGowan et al. (2019a) by calculating the center of mass (i.e. the mean vertical location within a 0.5 km horizontal bin weighted by s_A) depth within 25 m bottom depth increments for summer and fall.

2.6. Population dynamics

To examine trends in relative abundance of capelin in the GOA, we compared annual estimates of mean densities of larval and age-1+ fish from offshore surveys. Indices were calculated from each of the following data sources: mean CPUEs for larval capelin (no. fish 10 m^{-2}) from the EC survey (fall samples only); mean CPUEs for age-1+ capelin (kg km^{-2}) from the BT, MT (night samples only, cf. McGowan et al. 2019b), and AT surveys. Regional indices of relative abundance were derived for each index for years in which 8 or more samples were collected within a region (see Tables S3–S6). Time series from 2 additional data sources (see Supplement 1 for details) were included in the population dynamics analysis: larval capelin biomass collected during oceanographic sampling in fall along the Seward Line (Fig. 1) in the NGOA (hereafter SL survey), and an index of capelin relative abundance derived from prey compositions of various piscivorous seabird and groundfish species in the GOA using dynamic factor analysis (hereafter capelin DFA index). To facilitate direct comparisons among indices that are based on different sampling approaches, each survey-based index was standardized by subtracting index values from their mean and dividing by 1 SD. Consistency among the indices was assessed based on the direction and magnitude of anomalies.

2.7. Identifying core areas

Distributions from all inshore and offshore surveys were synthesized to identify areas that are consistently occupied by capelin in the GOA. High-density spawning habitat areas were identified based on the upper 90% density percentile for ShoreZone coastal habitat data using the restrictive classification criteria (see Table 1). To identify areas where larval and age-1+ capelin consistently occur, each inshore and offshore survey's distribution of normalized CPUEs was constrained to grid cells with values in the upper 50% density percentile, and then the retained grid cells from all of the surveys were combined by life stage and plotted as a composite distribution. Larval capelin distributions from summer and fall surveys were plotted separately to show seasonal differences. Core areas where age-1+ capelin concentrate were identified by concentrations of grid cells with normalized CPUE values in the upper 75% density percentile for any of the surveys. To improve visualization of the composite distributions, smooth polygons were created around the perimeters of clustered grid cells.

3. RESULTS

3.1. First year of life

3.1.1. Characterization of potential spawning habitat

Both permissive and restrictive criteria resulted in classifications of ubiquitous and abundant capelin spawning habitat (Fig. 2B,C) that was primarily distributed along coastlines that consisted of relatively flat, intertidal beaches comprised of sand and gravel, that were protected or semi-protected from wave exposure (Table 1). Permissive criteria identified 0 to 356.6 km of coastline per 1600 km^2 grid cell as poten-

tial spawning habitat, and restrictive criteria identified 0 to 77.5 km of coastline per cell, relative to a total coastline length per cell that ranged from 0 to 646.2 km. Habitat index density values varied between 0 and 1 and had a log-normal distribution (Fig. 2B,C), with most cells having a low density of potential spawning habitat. The spatial pattern of cells with the highest densities was similar between the permissive and restrictive scenarios, except that clusters of high-density cells were larger for the permissive criteria. Kodiak, the south Kenai Peninsula, western Prince William Sound, and southeast Alaska were determined to have substantial availability of potential spawning habitat. The 2 scenarios diverge somewhat in Cook Inlet: the restrictive criteria suggested high densities only in the northern part of the Inlet, while the permissive criteria suggested that spawning habitat is located throughout the area.

3.1.2. Simulated larval transport

The IBM results suggest broad-scale dispersal of capelin larvae across the GOA and connectivity between eastern spawning locations and the WGOA throughout the 6 mo modeled time period (Fig. 3).

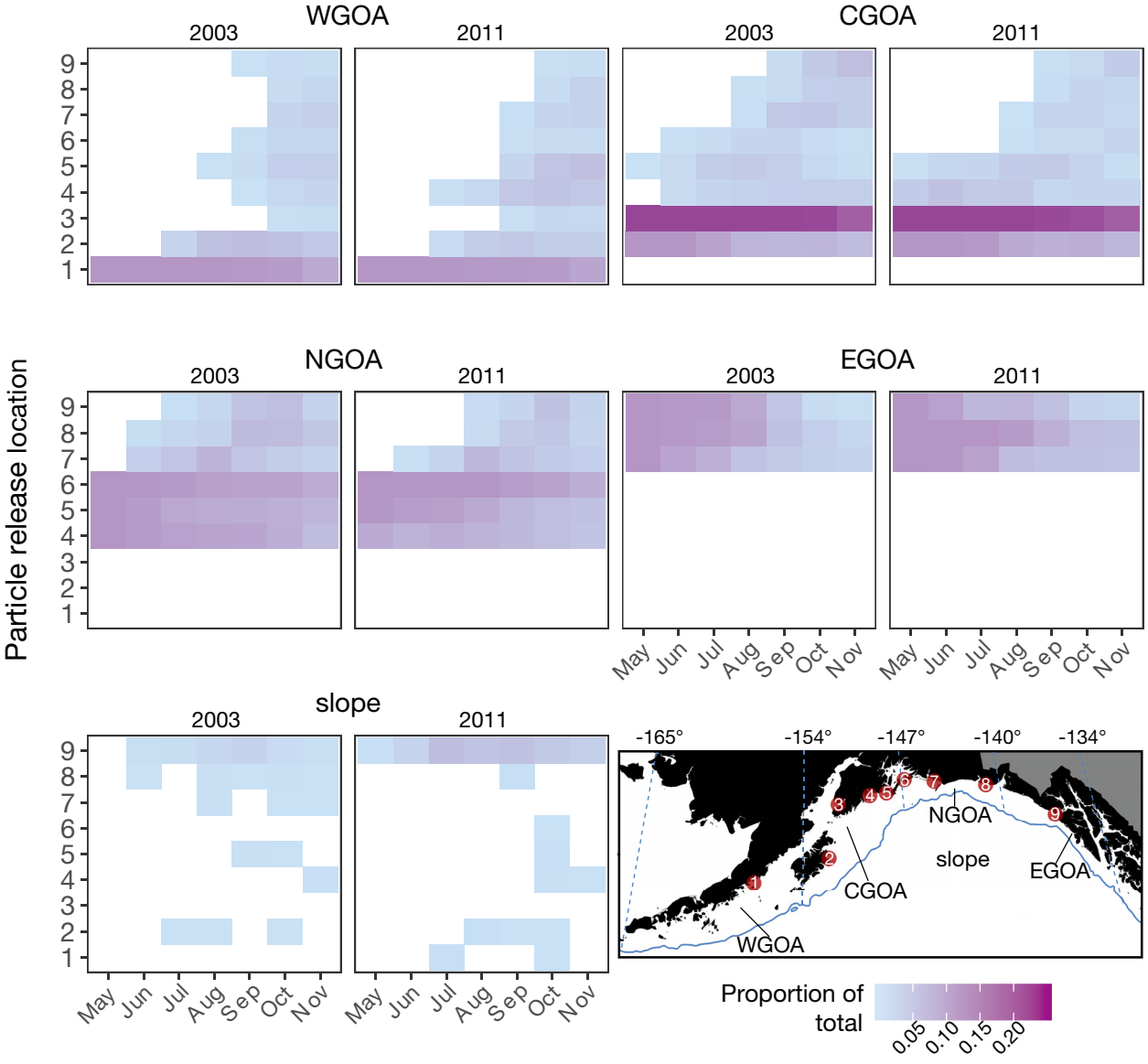

Fig. 3. Summary of simulated particle accumulation in 2003 and 2011 by month for each region of the Gulf of Alaska (GOA): areas of the western (WGOA), central (CGOA), northern (NGOA), and eastern (EGOA) continental shelf (<500 m), and waters deeper than 500 m (slope). The *y*-axis rows correspond to the particle release point locations indicated on the map by red circles (1–9). The solid blue line on the map shows the 500 m isobath

The degree to which particle accumulation within regions in the GOA can be attributed to a single or an amalgam of spawning locations differed among regions and across months. For example, particles from all spawning locations contributed to capelin larval occurrence in the WGOA, but larvae spawned in spring or summer (May, June, July) in the EGOA (i.e. Cross Sound, location 9) may not reach the WGOA until November. In contrast, those spawned in the WGOA (Alaska Peninsula, location 1) contributed substantially to larval abundance in the region throughout all months. Interestingly, larvae accumulating in the CGOA were primarily sourced from Kachemak Bay (location 3), indicating high retention of larvae spawned within Cook Inlet. In contrast to these more westward regions in the GOA, larval occurrence and accumulation in the NGOA and EGOA regions could not be attributed to a single spawn location to the same degree. Notably, larval occurrence in the EGOA was the result of spawning near the Copper River (location 7), between Icy Bay and Yakutat Bay (location 8), and Cross Sound, indicating eastward transport of particles from the Copper River. Though few particles were transported to the slope region, most were released from Cross Sound.

Comparisons among spawning months indicated that differences in spawn timing also impact larval trajectories. For example, in both 2003 and 2011, particles released in May from Prince William Sound–Montague Strait (location 5) traveled to the south of Kodiak in comparison to the other 2 spawning months (Fig. 4). In contrast, there were minor differences in larval trajectories between 2003 and 2011, during which particles in both years traversed across the GOA shelf and were primarily transported through Shelikof Strait via the Kennedy-Stevenson Entrance to the north of Kodiak (Figs. S3 & S4 in Supplement 3). This pattern was also emphasized by the scarcity of particles found in the slope region across any of the study months (Fig. 3). These transport paths were clearly related to circulation patterns over the GOA shelf (Fig. 1). Notable differences among years included a greater number of larvae offshore in 2011 compared to 2003 that were spawned from Cross Sound and some differences in divergences of particle transport to the north and south of Kodiak (Fig. 4).

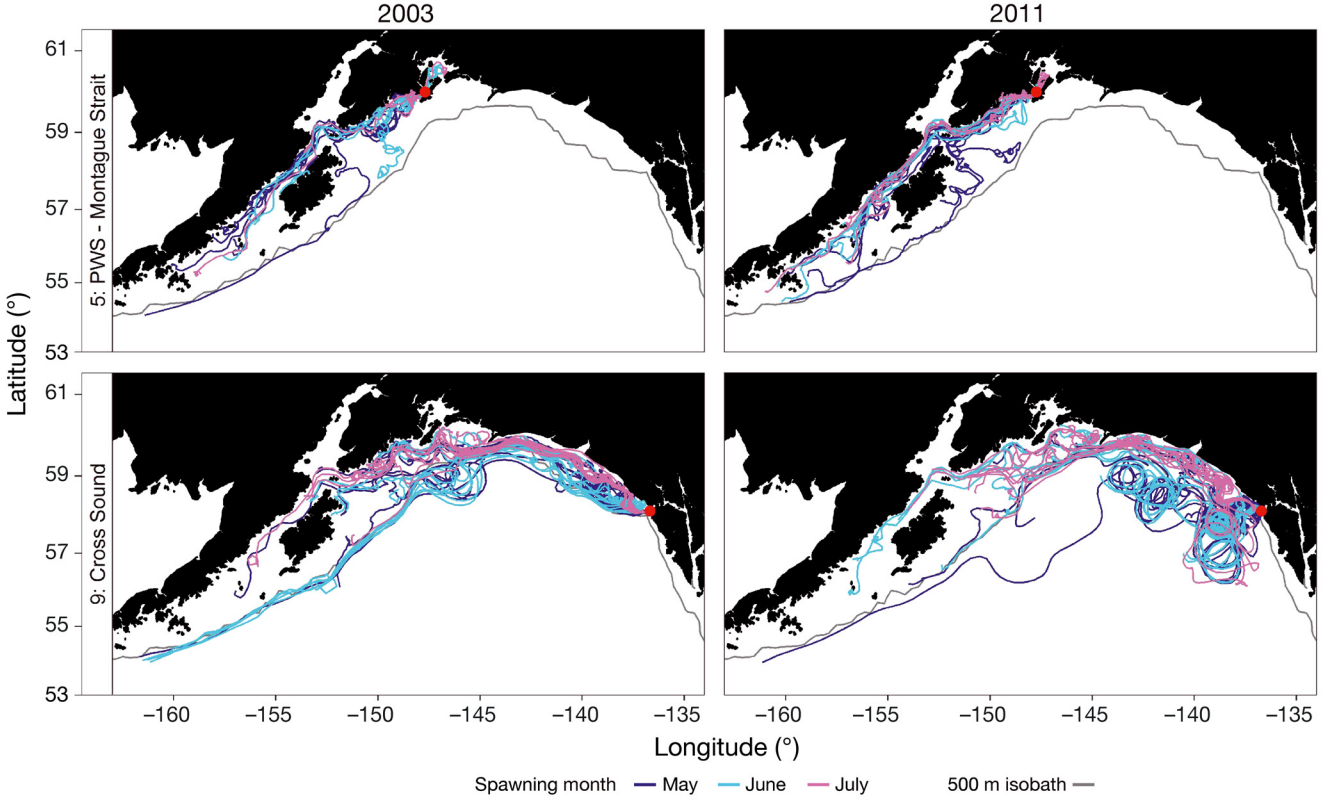

Fig. 4. Simulated trajectories presenting the daily model output across the 6 mo duration of the model in 2003 and 2011 from the Prince William Sound (PWS)–Montague Strait and Cross Sound spawn locations (red circles). Particles were released daily from the 10th to the 20th day of each month.

3.2. Spatial dynamics

3.2.1. Larval distributions

Inshore distributions of capelin larvae were patchy during summer in SCAK (Fig. 5, Table S2), primarily occurring in western and northern Prince William Sound, with low frequency of occurrence in Cook Inlet. In contrast, capelin larvae were more widely distributed in SEAK, where high densities occurred in Glacier Bay, Cross Sound, Icy Bay, and Yakutat Bay. Length frequency distributions of larvae in the SCAK region peaked between 2.0 and 3.0 cm L_S, whereas we observed no well defined peaks across a wider distribution of lengths between ~2.0 and 4.5 cm L_S in SEAK (Fig. 5).

Overall, the density of larval capelin offshore was higher over the inner shelf and consistently low near or beyond the shelf break (Fig. 6). In spring, larval capelin were rarely caught (Table S3), with most occurrences observed along the southern edge of Kodiak. Length composition in spring indicated relatively large larvae, often greater than 3.0 cm L_S, suggesting that these fish were spawned the prior year. In the summer, the highest densities of larval capelin were primarily nearshore in the EGOA and over the inner shelf in the CGOA. Larval densities in the summer were relatively low over the WGOA shelf, with exception of isolated high densities near the west side of Kodiak. Among the 3 seasons, larval capelin were smaller in the summer, with the majority being between 0.5 and 1.0 cm L_S. Frequency of occurrence and densities of larval capelin were highest in fall (Table S3), with the highest densities observed nearshore of Kodiak. Although some high-density patches of larval capelin were observed along the Alaska Peninsula, densities were generally lower in the WGOA compared to the CGOA (but note that there was limited survey coverage in the NGOA and EGOA regions in fall). Larvae had a wider size distribution in the fall (most between 1.0 and 1.5 cm L_S) than in summer, suggesting a protracted spawning period and/or spatially variable growth rates.

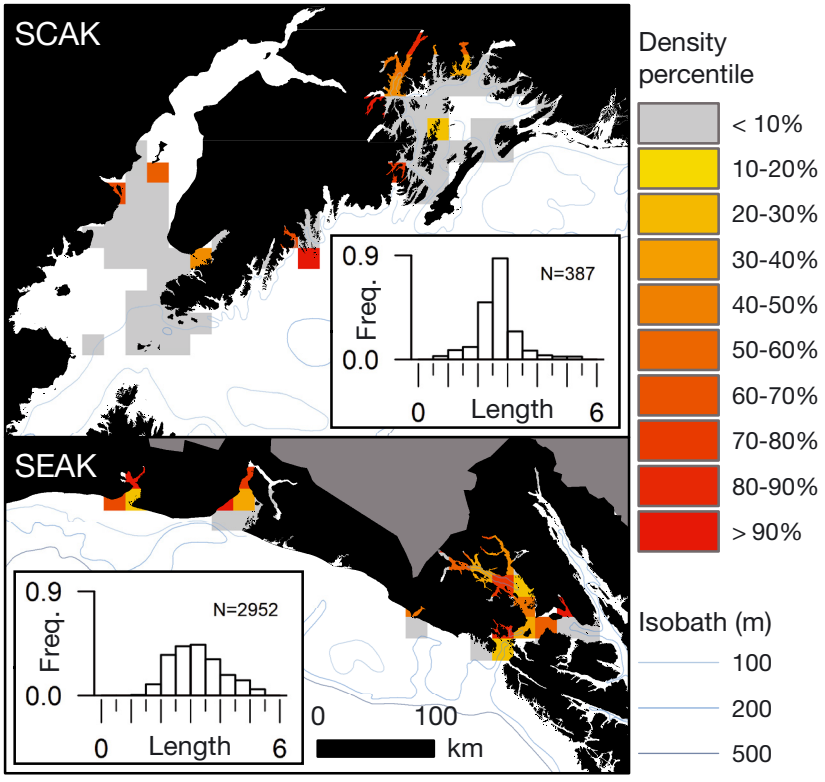

Fig. 5. Inshore distributions of normalized density percentiles and relative length frequency (insets; standard length, cm) of capelin larvae in 1996 to 2016 by region: Southcentral Alaska (SCAK), Southeast Alaska (SEAK)

3.2.2. Age-1+ distributions

Inshore densities of age-1+ capelin in summer were concentrated on the western side of Cook Inlet, the mouth of Kachemak Bay, and along the Barren Islands. They were also concentrated near tidewater glaciers in Kenai Fjords, Prince William Sound, Icy Bay, Yakutat Bay, Lituya Bay, Glacier Bay, and Lynn Canal (Fig. 7). USGS surveys recorded maturity stage, observing capelin in spawning condition at all inshore sampling locations (Table S2) in the SCAK and SEAK regions during summer months. Similar to capelin larvae, length frequency distributions of age 1+ fish exhibited a peak between 7 and 9 cm L_F in SCAK while they were spread over a greater range of lengths (6 to 11 cm) in SEAK. Frequency of occurrence of subadult and adult capelin in trawls in SEAK (Cook Inlet: 11–35%; Prince William Sound: 0–42%) was generally lower and less consistent among years than in SEAK (especially Glacier Bay: 52–59%) (Table S2).

Offshore distributions of age-1+ capelin were consistently concentrated over the CGOA shelf near Kodiak (Fig. 8). High densities of capelin (>80% density percentile)

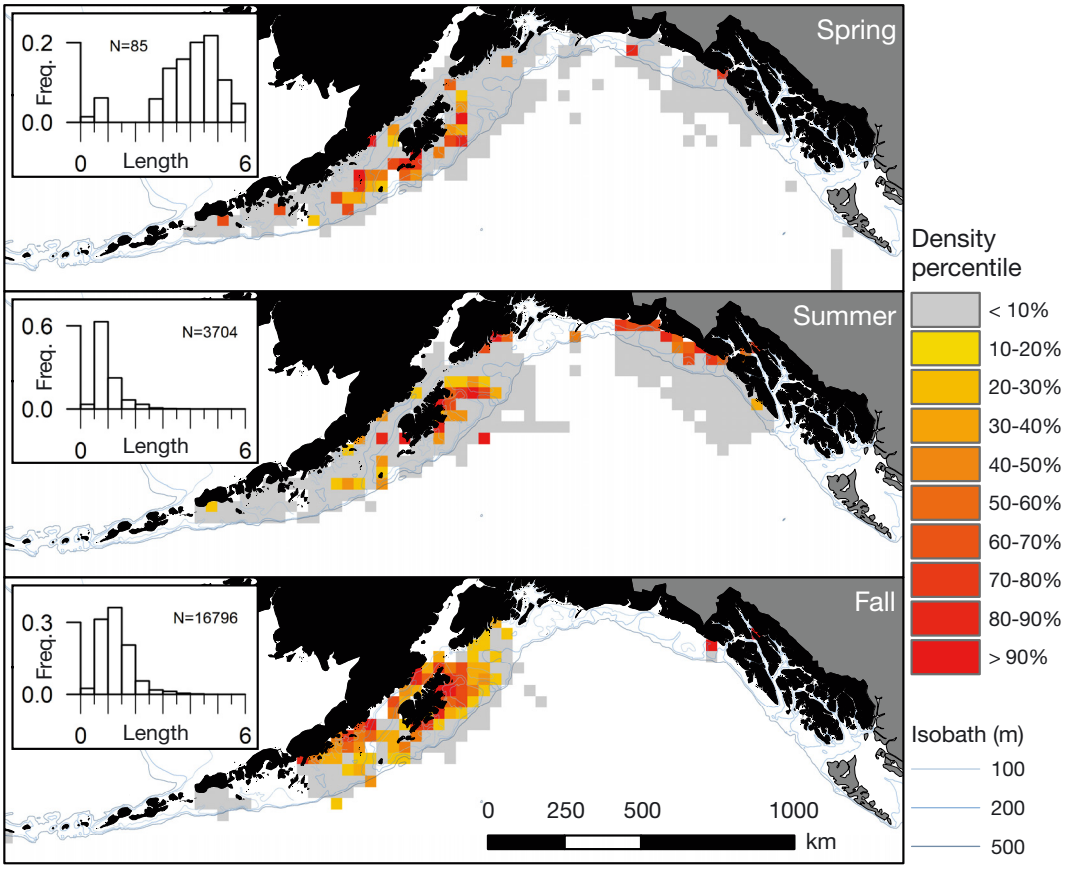

Fig. 6. Offshore distributions of normalized density percentiles and relative length frequency (insets; standard length, cm) of capelin larvae in 2000 to 2015 by season

occurred in the CGOA region over or near Albatross and Portlock Banks and north of Kodiak. In the WGOA, the BT and MT surveys observed high densities of capelin near Unimak Island, while the MT survey (and to a lesser extent the AT survey) measured moderate to high densities of capelin over the inner shelf along the Alaska Peninsula between the Shumagin and Semidi Island groups. In the NGOA, high densities of capelin were encountered both over the outer shelf near Middleton Island and the inner shelf near Kayak Island. In the EGOA, the BT survey sampled high densities of capelin along the coast between Yakutat and Cross Sound, with no aggregations observed over the shelf southeast of Cross Sound.

Length compositions from the age-1+ offshore surveys indicated 2 distinct length modes that ranged from 7 to 10 and 10 to 13 cm L_F (Fig. 8). Published length–age relationships indicate these modes correspond with age-1 and older fish; however, length is not a reliable way to age immature capelin (Pahlke 1985, Naumenko 1996). Both size modes were clearly observed in trawl catches from the AT and GE acoustic surveys. In contrast, the MT survey's catches were mostly comprised of smaller fish (7 to 9 cm), while the BT survey catches were comprised of larger fish (9 to 13 cm). These differences in length distributions are not surprising given that the MT survey uses a smaller net with a finer mesh liner in the codend (3 mm) compared to the other surveys (1.3 to 3.2 cm mesh codend liner).

CPUEs varied by orders of magnitude among the offshore surveys (Fig. 9). Annual averages of all samples where capelin were present (i.e. non-zero means) were lowest in the BT survey (range: 2.1 to 252.8 kg km^{-2}, Table S5), followed by the MT survey (day sample range: 20.4 to 1382.4 kg km^{-2}, night sample range: 10.4 to 2123.8 kg km^{-2}, Table S4), and highest in the AT survey (range: 5855 to 18 086 kg km^{-2}, Table S6). These differences are not surprising given that each of these surveys employs different sampling approaches. In contrast, non-zero acoustic densities from the AT (mean s_A ± SE: 657.8 ± 47.2 m^2 n mile^{-1}, range: 0.6 × 10^{-2} to 6.0 × 10^4 m^2 n mile^{-1}) and GE (mean s_A ± SE: 783.2 ± 65.1 m^2 n mile^{-1}, range: 1.7× 10^{-2} to 1.5 × 10^4 m^2 n mile^{-1}) surveys in 2013 were of similar magnitude.

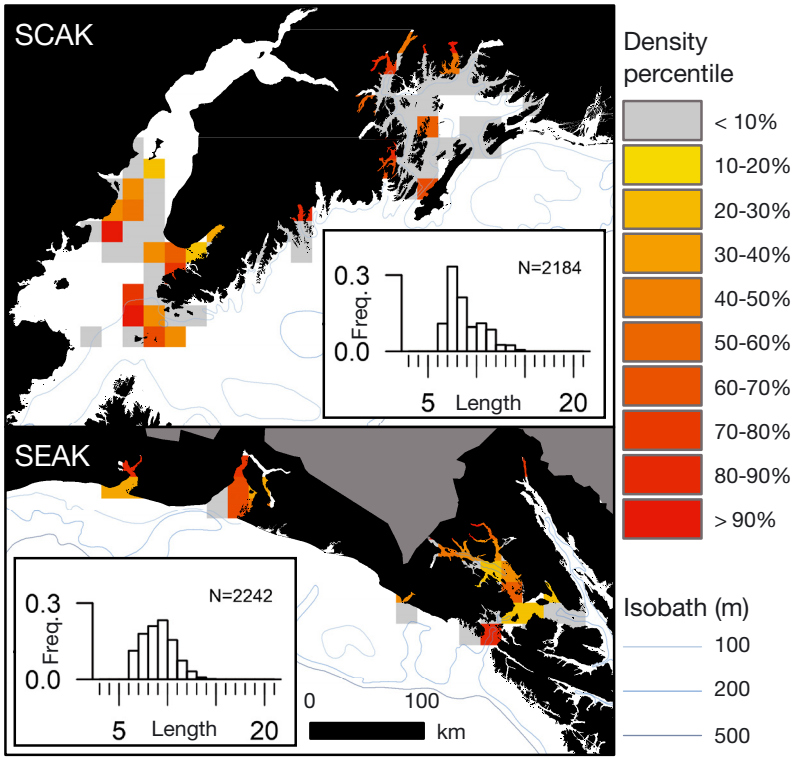

Fig. 7. Inshore distributions of normalized density percentiles and relative length frequency (insets; fork length, cm) of age-1+ capelin in 1996 to 2016 by region: Southcentral Alaska (SCAK), Southeast Alaska (SEAK)

3.2.3. Age-1+ distributions relative to bottom depth

There were differences in catch rates of age-1+ capelin relative to bottom depth among the surveys. The mean bottom depth of samples where capelin were present was shallowest in the BT survey (mean ± SE: 111 ± 2.0 m) and deepest in the MT survey (138 ± 3.7/134 ± 3.7 m for day/night samples) while both acoustic surveys ranged from 118 to 122 m (Fig. 9). In contrast, the MT survey sampled shallower waters (mean bottom depth for all samples: 130 ± 3.6/136 ± 4.1 m for day/night) compared to the area sampled by the BT (159 ± 1.6 m), AT (214 ± 1.2 m), and GE (311 ± 8.3 m) surveys (not shown). When weighted by capelin density, mean bottom depths shifted towards shallower depths in all surveys, and indicate that capelin primarily concentrate between depths of 80 and 120 m over the GOA shelf. In most years, the frequency of capelin occurrence was higher in shallow waters (<100 m bottom depth) compared to deeper waters (100–300 m) over the shelf during the BT and acoustic surveys (Fig. 10). The opposite pattern was observed in the MT survey during which occurrence frequencies were higher over deep shelf waters in all years except one (2000), particularly during the daytime.

Vertical distributions of age-1+ capelin from the daytime GE survey were clearly associated with bottom depth (Fig. 11), occupying vertical positions that were lower in the water column over deeper bottom depths. Capelin occupied a wide range of water column depths in summer (center of mass range: 13 to 149 m) and fall (range: 15 to 192 m). In both seasons, the mean (±1 SD) center of mass was shallowest over bottom depths less than 75 m (51.3 ± 12.0 m in summer; 47.8 ± 15.5 m in fall) and gradually descended to lower vertical depths over deeper waters of the shelf. Across all depths, capelin were located closer to the seafloor than the surface. Over shallow waters (<100 m bottom depth), the mean distance between the seafloor and capelin center of mass was <20 m in both seasons (18.6 ± 16.4 m in summer; 18.3 ± 14.8 m in fall). In comparison, the mean (±1 SD) seafloor to center of mass distance was 36.8 ± 21.4 m in summer and 23.8 ± 13.8 m in fall between 100 and 150 m, and greater than 45 m in both seasons over deeper bottom depths.

3.3. Population dynamics

Interannual fluctuations in the relative abundance of capelin occurred between 2000 and 2015, but years in which abundance was high or low varied among the 6 indices (Fig. 12). Above-average capelin abundance was most evident in 2013 when positive anomalies occurred in 5 of the 6 indices, of which 4 were strong anomalies (standardized index value >1). Below-average abundance was apparent in 2015 when negative anomalies occurred in all indices that reported CPUEs, including strong anomalies (< −1) in the EC, BT, and MT surveys; in addition, capelin abundance was too low for the AT survey to estimate capelin backscatter in 2015. Low capelin abundance also likely occurred in 2000 and 2001, when negative anomalies were evident in a majority of the indices. For other years, inconsistencies among index values make it difficult to evaluate trends in capelin abundance. The sign of anomalies from the larval indices of abundance for the GOA only matched during 3 of

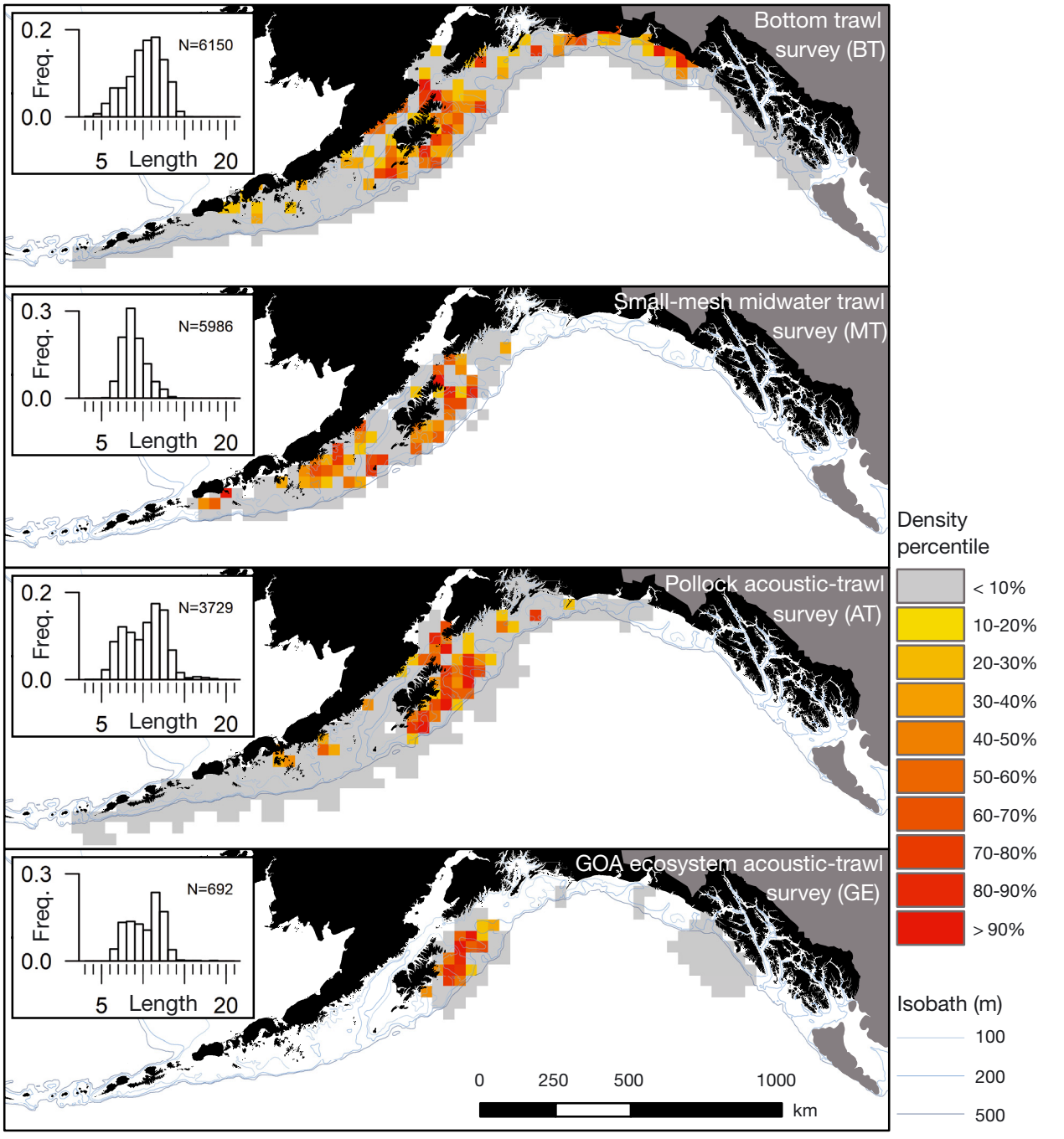

Fig. 8. Offshore distributions of normalized density percentiles and relative length frequency (insets; fork length, cm) of age-1+ capelin by survey (coverage period): BT (2001–2015 odd years); MT (2000, 2001–2015 odd years); AT (2003, 2005, 2011, 2013); GE (summer 2013)

the 11 yr (2000, 2013, 2015) for which data were available from both the EC and SL surveys. Among the age-1+ surveys, GOA abundance anomalies were similar among the BT and AT surveys in all years, and suggest that capelin abundance was also above average in 2003. In contrast, anomalies from the MT survey were only consistent with the BT survey in 2 of 8 yr (2001, 2015), although these differences may be attributed to high variances around mean CPUEs from the MT survey. The sinusoidal trend in the capelin DFA index, which reflects relative availability to piscivorous predators, was not observed in the survey-based indices, but anomalies were similar to the SL survey in 11 of 16 yr.

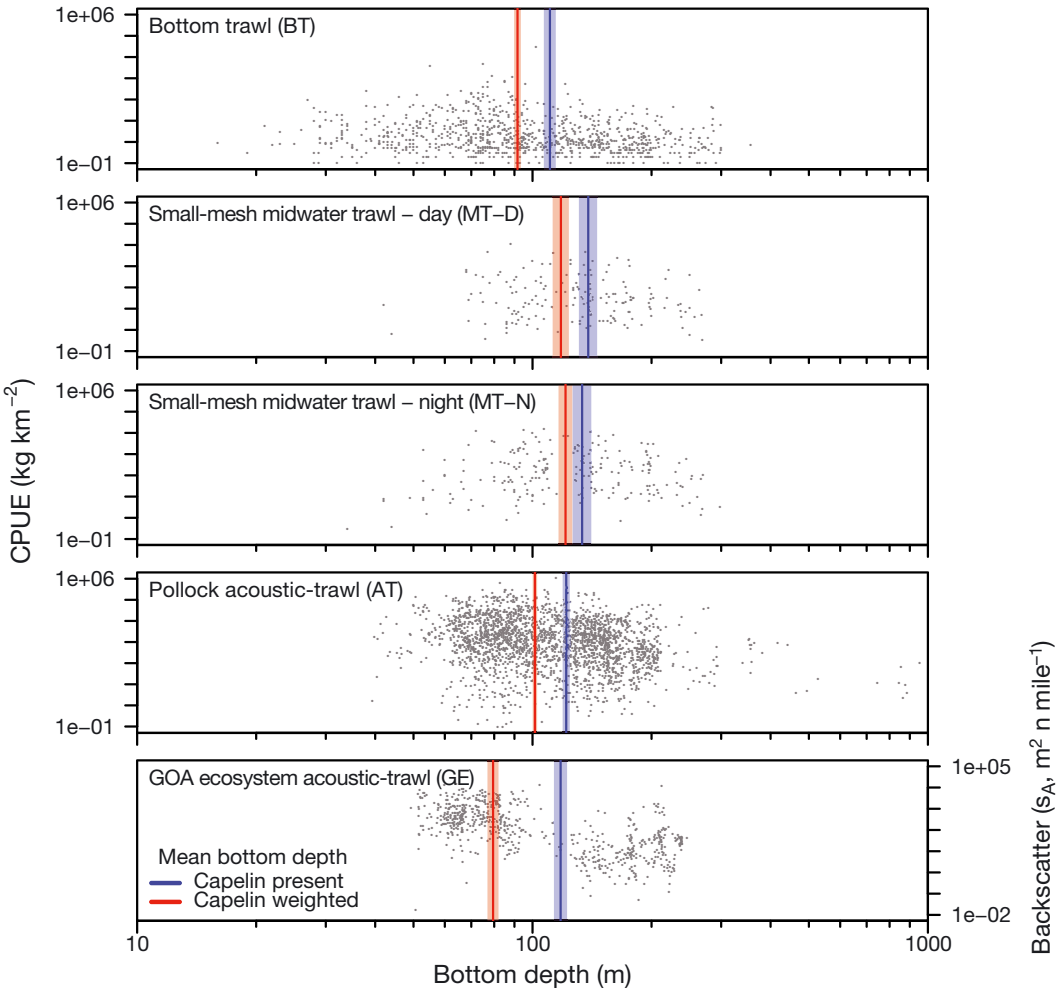

Fig. 9. Density of age-1+ capelin relative to bottom depth for the offshore surveys. Catch per unit effort (CPUE) for biomass (kg km^{-2}) is on the left axis and acoustic backscatter attributed to capelin (s_A, m^2 n mile^{-1}) is on the right axis for the GE survey. Mean bottom depths were calculated as: 'capelin present' = samples in which capelin CPUE > 1; 'capelin weighted' = mean depth weighted by capelin CPUE. Shaded areas indicate 95% confidence interval for the mean

Inter- and intraregional differences in abundance trends were also apparent among the larval and age-1+ indices. In the EC survey, mean densities of larval capelin were higher in the CGOA region compared to the WGOA in all years that 8 or more samples were collected in both regions (Table S3). Similarly, mean and non-zero mean CPUEs from all age-1+ surveys were highest in the CGOA region in most years (Tables S4–S7). For example, abundance trends from the BT survey for the GOA were driven by higher non-zero mean CPUEs from the CGOA region (Table S5) and did not match trends observed in the WGOA and NGOA regions (Fig. 12). In the MT and AT surveys, differences in abundance trends between the WGOA and CGOA regions occurred in a majority of years (Tables S4 & S6), yet these pronounced regional differences were partially obscured when CPUEs were averaged across the GOA. Despite high interannual and spatial variability among the surveys, capelin were consistently observed in CGOA waters near Kodiak in all offshore surveys prior to 2015 (Tables S3–S7).

3.4. Conceptual model of distributions

Capelin distributions from inshore and offshore surveys were synthesized by life stage to create composite maps of areas consistently occupied by capelin in the GOA (Fig. 13). Potential capelin spawning habitat is primarily concentrated within 4 areas of the GOA: islands in the WGOA between Unimak Pass and the Shumagin Islands, Kodiak, the Kenai Peninsula coast and western Prince William Sound, and

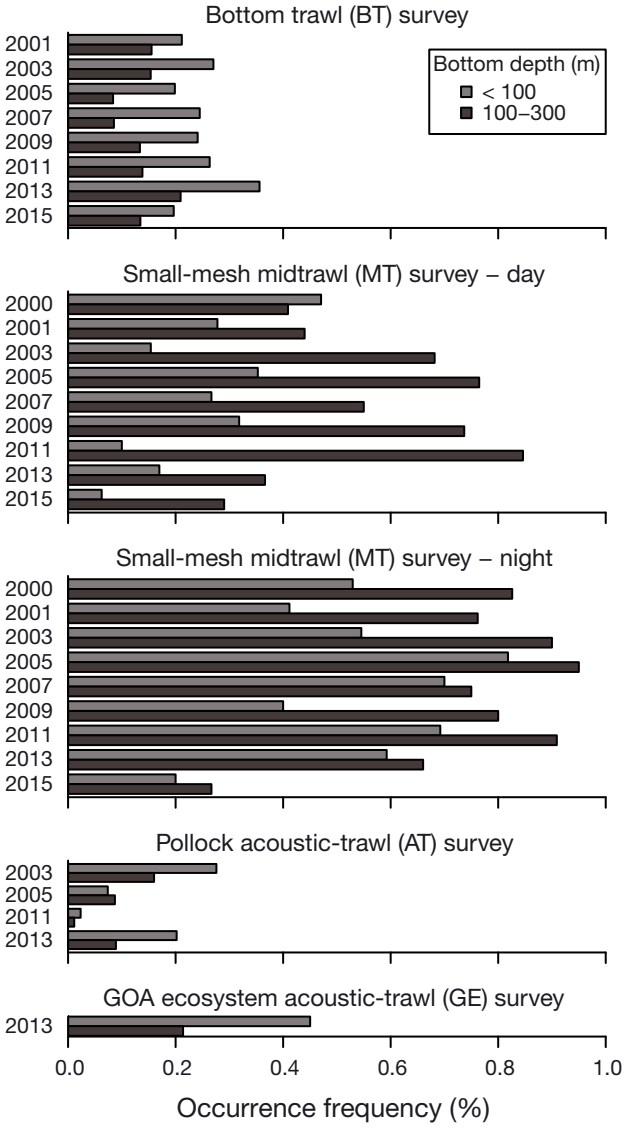

Fig. 10. Occurrence frequencies for age-1+ capelin by year and bottom depth strata (<100 m = shallow shelf, 100–300 m = deep shelf) for the offshore surveys. Years with fewer than 8 samples are not shown, and samples from bottom depths >300 m are not shown

southeast Alaska. Although ShoreZone data are not available for Glacier Bay, we also identified this region as being an important spawning area within SEAK based on Arimitsu et al. (2008). Larval distributions in summer and fall are adjacent or just downstream of these spawning areas over the inner part of the GOA shelf. Larval capelin primarily occupy shelf waters near Kodiak in summer and fall, expanding their distributions downstream over the inner WGOA shelf in fall. The IBM trajectories indicate that these areas likely receive larvae from local spawning locations and from spawning areas located upstream in the NGOA, and to a lesser extent in the EGOA (Fig. 3; Figs. S3 & S4). Larval capelin also occupy coastal waters over the EGOA shelf and inshore waters of northern SEAK in summer, although what appears to be a seasonal reduction in larval distributions in fall in the EGOA may be an artifact due to a lack of fall ichthyoplankton surveys in this region (Fig. 6).

Concentrations of age-1+ fish over the shelf near Kodiak and lower Cook Inlet indicate that this area represents the core habitat of the GOA population. High spatial overlap between distributions of larval and age-1+ fish around Kodiak suggest that capelin settle in this area by fall of their first year. Similar overlap of small concentrations of age-1+ fish with broader distributions of larval capelin in the EGOA suggest that capelin may also settle earlier in summer near local spawning areas. In contrast, small concentrations of age-1+ capelin near Unimak Island in the WGOA did not overlap with observed larval distributions, suggesting movement by age-1+ fish to this area. Limited sampling in the NGOA by the EC survey (Fig. 6) prevented comparison of larval distributions with aggregations of age-1+ capelin located near Middleton Island.

4. DISCUSSION

4.1. Core areas for capelin in the GOA

For at least the past 2 decades, capelin in the GOA have primarily concentrated over shelf waters near

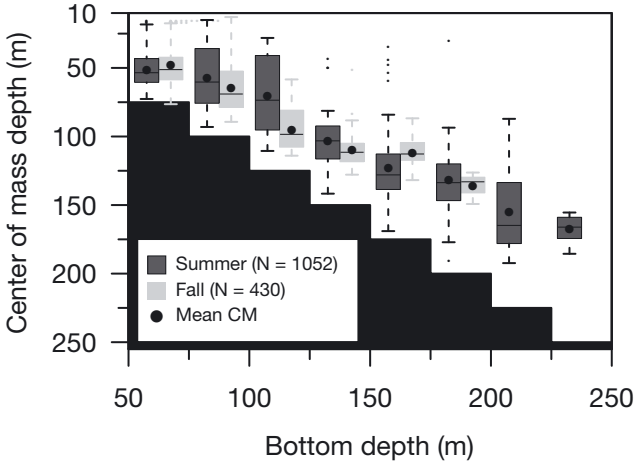

Fig. 11. Vertical distributions of age-1+capelin, represented by the center of mass (CM) depth within 25 m bottom depth increments for summer (August) and fall (September to October) from Gulf of Alaska ecosystem acoustic-trawl (GE) surveys in 2011 and 2013. Closed circle is the mean, solid line is the median, shaded area is the interquartile range (IQR), whiskers are 1.5 times the IQR, points are outliers

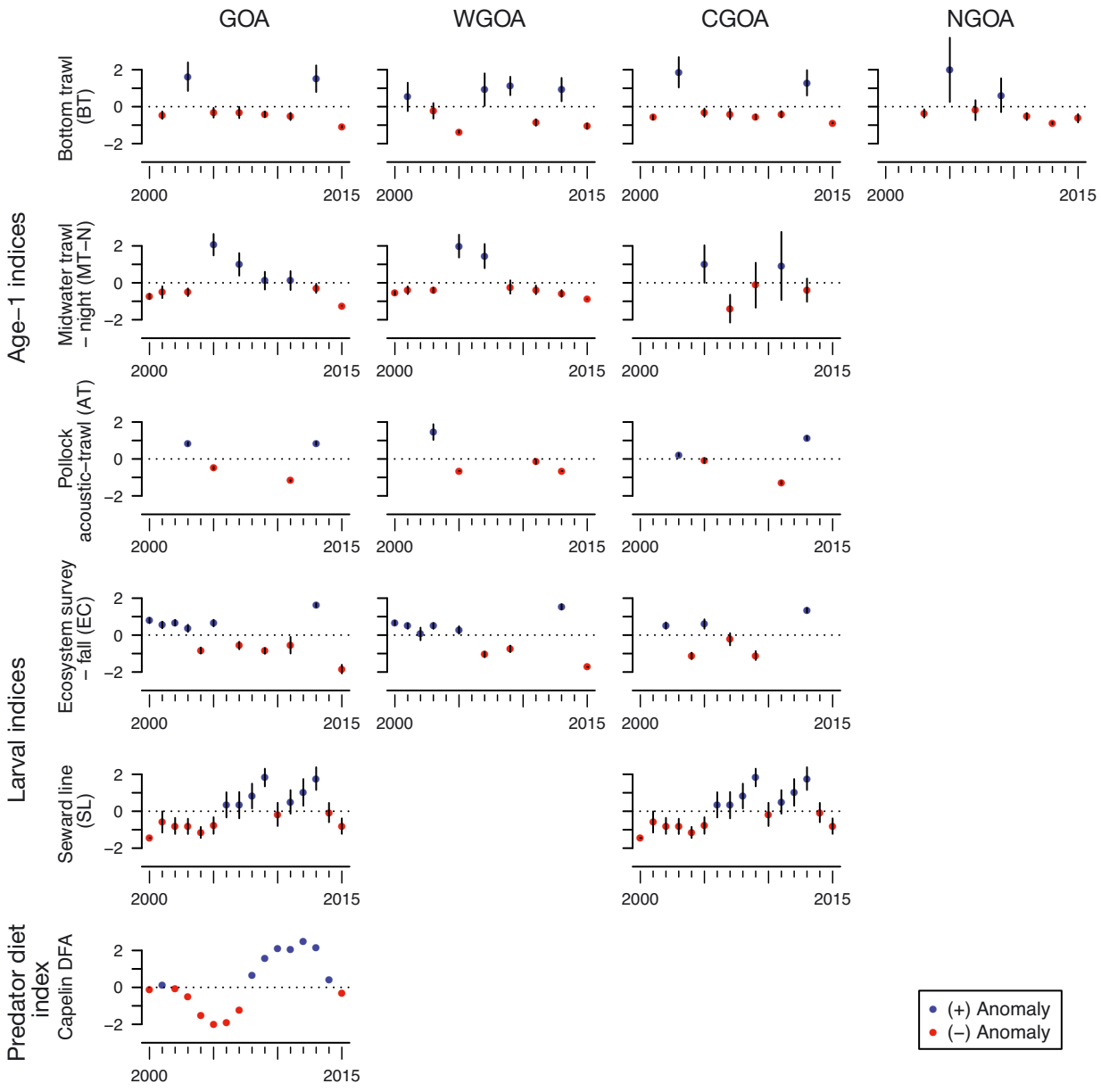

Fig. 12. Time series of capelin relative abundance in the Gulf of Alaska (GOA) and by offshore region: western (WGOA), central (CGOA), and northern (NGOA). Indices of relative abundance are shown for age-1+ capelin mean catch per unit effort (CPUE) from 3 surveys, larval capelin mean CPUE from 2 surveys, and anomalies for the predator diet-based capelin index. Years with fewer than 8 samples are not shown. Note that mean CPUEs are normalized, but not corrected for potential spatial autocorrelation, and standard errors of the mean should be interpreted with caution. DFA: dynamic factor analysis

the Kodiak Archipelago. The consistent occurrence of high CPUEs of larval and age-1+ capelin in waters around Kodiak can be attributed to the area's physical and biological features that facilitate larval retention from local and upstream spawning locations to the north and east, and relatively high and sustained production from spring to fall that promotes prey availability to capelin. IBM results show that larval capelin can be transported across the shelf from east to west within a 6 mo period by the ACC. Where the ACC bifurcates at Kennedy-Stevenson Entrance in the CGOA (Fig. 1), larvae are either advected into the WGOA through Shelikof Strait or to the south along the eastern side of Kodiak. Current velocities on the shelf along the east–southeast side of Kodiak (hereafter the Kodiak shelf) are generally weak in summer compared to much of the GOA shelf (cf. Fig. 4 in Stabeno et al. 2016a). Weak currents and eddy-like circulation around submarine banks (Stabeno et al. 2004, Ladd et al. 2005, Cheng et

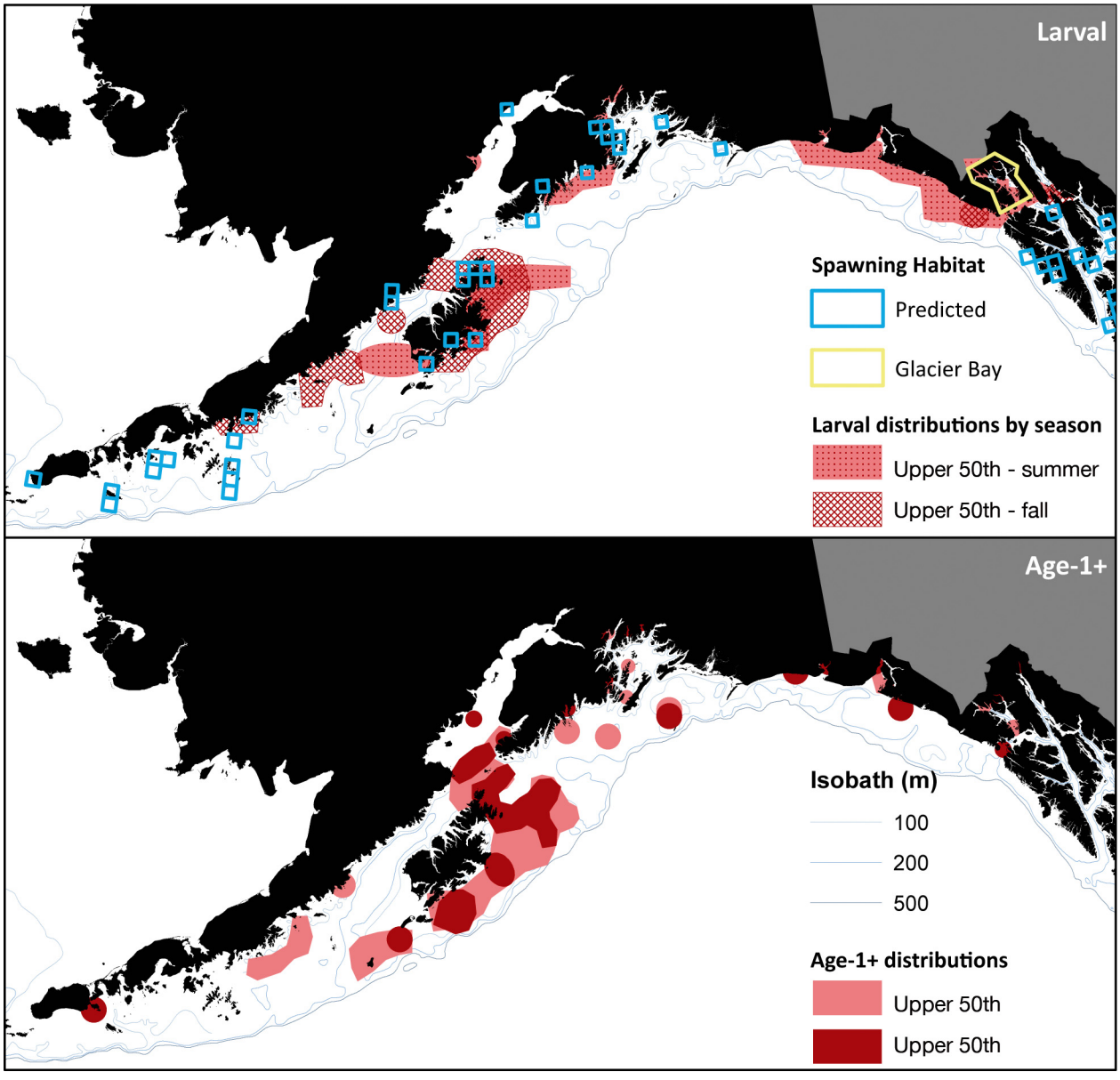

Fig. 13. Conceptual diagram of areas that are consistently occupied by capelin. (A) Potential capelin spawning habitat based on the upper 25th log-normalized quartile using restrictive classification criteria (see Table 1), and larval distributions in summer and fall based on the upper 50th density percentile of catch per unit effort (CPUE). Glacier Bay is also identified as a spawning area based on Arimitsu et al. (2008). (B) Distributions of age-1+ capelin based on the upper 50th density percentile of CPUEs, with core areas indicated by the upper 75th percentile

al. 2012) may enhance retention of fish larvae over the Kodiak shelf (Mordy et al. 2019) and accumulate fish larvae from spawning locations in the CGOA and EGOA regions (Goldstein et al. 2019). With the potential for local and upstream spawning areas (i.e. Kenai Peninsula, western Prince William Sound, and SEAK) to supply larvae to the Kodiak shelf throughout the summer and fall, this area may represent the collective spawning output of much of the GOA population.

Bathymetric and circulation features of the Kodiak shelf are also likely to contribute to increasing the availability of prey to larval and age-1+ capelin through summer and fall. Satellite (Waite & Mueter 2013, Stabeno et al. 2016a) and model-based (Coyle et al. 2019) measures of integrated chlorophyll-α show that primary production is higher over the Kodiak shelf, in Shelikof Strait, and lower Cook Inlet from June through October compared to most of the GOA, where productivity is greatly reduced follow-

ing the spring bloom in April–May. Primary production over the shelf is nitrate-limited in summer (Strom et al. 2006), yet is sustained over the Kodiak shelf by strong tidal pumping that supplies nitrate from bottom water to the euphotic zone (Ladd et al. 2005, Cheng et al. 2012, Mordy et al. 2019). Production is locally enhanced over and near banks due to increased vertical mixing that results from the interaction of tidal currents and the ACC with steep walls along troughs (Stabeno et al. 2016a, Mordy et al. 2019). Increases in ACC transport, which supplies shelf waters with terrestrial-derived iron delivered from river discharge, further enhances production (Stabeno et al. 2004, Lippiatt et al. 2010, Cheng et al. 2012). The extended production period in Kodiak waters likely increases availability of micro- and mesozooplankton prey when zooplankton biomass declines over much of the shelf following the spring bloom (Coyle & Pinchuk 2005, Coyle et al. 2013). Although zooplankton availability declines seasonally (Wilson et al. 2005), the Kodiak shelf supports high late-summer densities of large euphausiids (Wilson et al. 2013) that are preferred prey of age-1+ capelin (Wilson et al. 2006).

Primary production is also higher in other areas of the GOA where larval and age-1+ capelin concentrate in smaller patches, indicating a potential link between productivity and capelin distributions and abundance. Satellite imagery from summer shows elevated production over the shelf near Montague Strait and north of Cross Sound (Waite & Mueter 2013, Stabeno et al. 2016a,b) where capelin larvae concentrate. *In situ* measures of integrated chlorophyll *a* also show that high summer production is sustained in the inshore waters of Cross Sound and Glacier Bay (Etherington et al. 2007) where larval and age-1+ capelin concentrate (Fig. 13; Arimitsu et al. 2008). Sustained production over the EGOA shelf north of Cross Sound is fueled by nutrients supplied from increased mixing within the Sound (Stabeno et al. 2016b). Production is also higher in summer and fall near Montague Strait, as well as near Middleton Island (Coyle et al. 2019) where age-1+ capelin were locally concentrated. Waters around Middleton Island are commonly associated with shelf-break eddies, which can move nitrate onshore and iron offshore (Coyle et al. 2019). The importance of these core areas is supported by the IBM larval dispersal simulation that shows transport and trajectories that encompass these regions, as well as accumulation of larvae within these areas of weaker currents and high primary productivity. This indicates that areas of the GOA shelf with sustained and elevated primary production serve as pelagic essential fish habitat for capelin and potentially other pelagic fishes.

This study's composite spatial pattern for age-1+ capelin is similar to distributions based on diets of capelin predators sampled in the GOA and Aleutian Islands. Piatt et al. (2018) characterized spatial patterns of capelin and other forage species using thousands of bill load data collected from tufted puffins *Fratercula cirrhata* located at 35 colonies between 1978 and 2013, and stomach content data from groundfish (i.e. gadids and flatfishes) sampled during the BT survey between 1990 and 2012. Both predator-based distributions show that the highest consumption of capelin occurred over the Kodiak shelf and in lower Cook Inlet, with more localized areas also occurring in the WGOA dispersed between Unalaska Island and the Semidi Islands, in the NGOA near Middleton Island and southwest Prince William Sound, and in the EGOA near Sitka Sound (cf. Fig. 5 in Piatt et al. 2018).

4.2. Spatio-temporal trends in capelin abundance

Previous work in the NE Pacific suggests that capelin populations respond to ocean temperatures. Anderson & Piatt (1999) attributed the decline of capelin in the GOA to the onset of warmer ocean conditions that followed the late 1970s regime shift (Francis et al. 1998). In more recent years, expanded distributions of capelin and/or increases in their relative abundance coincided with cooler temperatures in the GOA (Mueter & Norcross 2002, Hatch 2013, Sydeman et al. 2017) and eastern Bering Sea (Andrews et al. 2016). In this study, index values show high capelin abundance in 2013, coinciding with the end of a period of cold years (2008–2013), and very low abundance levels in 2015 during the peak of the recent marine heatwave (2014–2016) (Bond et al. 2015, Zador & Yasumishii 2017). Anomalously warm conditions are likely to be a contributing factor to low capelin abundances in 2015. These observations support the hypothesis that boreo-Arctic fish species such as capelin are vulnerable to large-scale warm temperature anomalies. This vulnerability may increase as the frequency and magnitude of marine heatwaves are predicted to increase in the North Pacific (Oliver et al. 2018).

In other years between 2000 and 2011, a period of less extreme shifts between relatively warm and cold years in the GOA, all index values are highly variable and capelin abundance trends are less clear. These observations are not consistent with the idea

that biomass variations are directly tied to changes in GOA ocean temperatures. Relatively high abundances were observed during the 2003 AT and BT surveys, and the 2005 MT survey coincided with warmer ocean temperatures, while low abundance levels were observed during cooler years in the BT (2007–2011) and AT (2011) surveys. Overall, the available observations indicate that capelin biomass levels are highly variable in the GOA, especially in areas located outside the CGOA region, and that our understanding of environmental linkages to capelin population dynamics in the NE Pacific remains limited. At the same time, inconsistencies among these time series in some years highlight the limitations of monitoring abundance trends using data from surveys not designed to sample capelin or other small pelagic fishes. Contradictory abundance index values were not surprising given the differences in survey gears and designs, recognizing that the strength of combining multiple data sources was the emergence of spatial patterns, as well as identification of factors that potentially affect data interpretation.

Recognizing the limitations of the available individual data series for tracking capelin abundance, our findings highlight spatial considerations necessary for interpreting trends from survey- and predator-based indices from the GOA. Abundance trends were often different between surveys with limited spatial overlap due to patchy capelin distributions, indicating the need to account for intra- and inter-regional differences in survey coverage among the data sources (cf. examples in D. W. McGowan et al. unpubl.). Similar spatial considerations are necessary when interpreting abundance trends from predator-based indices. In addition, the effect of capelin vertical distributions on their availability to different sampling gears and predators is related to bottom depth. For example, the close proximity of age-1+ capelin to the seafloor in shallow waters (<100 m bottom depth) during daytime likely increases their availability to bottom trawls, but potentially reduces their availability to midwater trawls. Conversely, increased distances between capelin and the seafloor over deeper waters likely reduces their availability to bottom trawls and increases their availability to midwater trawls (e.g. O'Driscoll et al. 2002). Furthermore, surface measures used to track changes in capelin distributions in other areas of the NE Pacific (Parker-Stetter et al. 2013, Logerwell et al. 2015, Andrews et al. 2016) are unreliable for the GOA because most capelin were located below the surface trawl footrope (~30 m) over the shelf. Similarly, the availability of capelin to surface-feeding predators is likely limited during the day over shelf waters deeper than 50 m bottom depth.

4.3. Implications for management of the GOA ecosystem

An improved understanding of how the environment influences recruitment and spatio-temporal variation in capelin densities is needed to better assess how GOA predators will be affected by future fluctuations in the availability of capelin and other forage species. There is strong evidence that predators have been impacted by rapid declines in capelin abundance following the late 1970s regime shift (Piatt & Anderson 1996, Merrick et al. 1997, Anderson & Piatt 1999) and the recent NE Pacific marine heatwave (Zador & Yasumishii 2017). The consistent occurrence of capelin in waters near Kodiak suggests that they provide a reliable prey source for predators compared to other regions where capelin abundance is more variable; this implies there is potentially a greater dependency on capelin for predators within the CGOA than in other GOA regions (Kettle et al. 2015, Piatt et al. 2018). However, similar sharp reductions of capelin in seabird chick diets at Middleton Island in the NGOA have also been documented during and after the marine heatwave (Hatch 2018), indicating that the effects of the recent decline in capelin abundance on predators are not limited to the CGOA. Therefore, anomalously low capelin densities around Kodiak in 2015 were likely the greatest reduction in prey supply in the past 2 decades, and preliminary analysis of survey data from 2017 indicates that capelin are still recovering in the CGOA and other GOA regions (Zador & Yasumishii 2017, Jones et al. 2019, D. W. McGowan et al. unpubl.).

To support an ecosystem-based approach to managing the GOA, improvements in monitoring capelin distribution and abundance are needed to provide managers with timely information on how the availability of this key forage species varies. This study identifies the Kodiak shelf and other core areas where monitoring efforts for capelin should be prioritized. Our findings also show that spatial considerations are necessary when interpreting abundance trends from survey- and predator-based indices of relative abundance. The available time series suggest that capelin densities in the GOA are highly variable across space and time. Thus, the impacts to predators in the GOA are spatially variable and dependent upon the predator's foraging strategy (e.g. central vs. non-central place foragers, shallow

vs. deep-divers). Knowledge of these variations can be used to assess trends and their potential impacts on managed species and other ecosystem components. In addition, we demonstrate that the limitations of data from individual surveys can be compensated for when integrated with additional data sources, and support future development of multivariate capelin abundance indices derived from spatially explicit survey and predator diet data sources.

To assess how capelin population dynamics and their availability to predators will be impacted by climate-related perturbations and long-term warming in the ocean (Hollowed et al. 2013), future research is needed to examine how capelin are affected by environmental variability during critical life stages. This includes (but is not limited to) assessing how spawning habitat selection and spawning distributions vary in space and time under different environmental conditions, relating spatio-temporal variations in larval densities with shifts in spawning distributions and larval transport trajectories, identifying key environmental factors that influence horizontal and vertical distributions of larvae and age-1+ capelin, and relating abundance indices with oceanographic and climate variables to better understand processes that drive recruitment dynamics.

4.4. Conclusion

Insights on the life history, distribution, and population dynamics of a non-commercial, but ecologically important species can be gained through an integrated analysis of modeled spawning habitat and larval dispersal with synthesis of spatially indexed data from multiple independent sources. We show that the core distribution of capelin in the GOA is located in the productive shelf waters surrounding the Kodiak Archipelago. Larval transport from inshore spawning locations distributed along the GOA coast to offshore shelf waters is primarily facilitated by the ACC and influenced by both the timing and location of spawning. Abundance indices from surveys and predator diets between 2000 and 2015 are highly variable and provide coherent trends only in recent years of relatively high (2013) and very low (2015) anomalies. With the goal of advancing ecosystem-based fisheries management in the North Pacific, monitoring strategies of Pacific capelin should consider the local-scale variability of GOA populations to improve assessments of the availability of forage species to predators.

Acknowledgements. We thank the officers, crew, and members of the scientific parties on NOAA-AFSC and USGS cruises that tirelessly collected survey data over the years. Special thanks to Janet Duffy-Anderson, whose support made this study possible, and to Dan Cooper for providing the larval capelin vertical distribution data. We thank A. Gallego, E. Logerwell, and 2 anonymous reviewers for providing comments that improved the manuscript. Funding was provided by the North Pacific Research Board, NOAA, and the 'Exxon Valdez' Oil Spill Trustee Council (EVOSTC). Any use of trade, firm, or product names is for descriptive purposes only and does not imply endorsement by the U.S. Government. The findings and conclusions of this paper do not necessarily represent the views of the National Marine Fisheries Service, NOAA, USGS, or EVOSTC. This research is contribution EcoFOCI-0937 to NOAA's Ecosystems and Fisheries-Oceanography Coordinated Investigations.

LITERATURE CITED

Abookire AA, Piatt JF (2005) Oceanographic conditions structure forage fishes into lipid-rich and lipid-poor communities in lower Cook Inlet, Alaska, USA. Mar Ecol Prog Ser 287:229–240

Anderson PJ, Piatt JF (1999) Community reorganization in the Gulf of Alaska following ocean climate regime shift. Mar Ecol Prog Ser 189:117–123

Andrews AG, Strasburger WW, Farley EV, Murphy JM, Coyle KO (2016) Effects of warm and cold climate conditions on capelin (*Mallotus villosus*) and Pacific herring (*Clupea pallasii*) in the eastern Bering Sea. Deep Sea Res II 134:235–246

Arimitsu ML, Piatt JF, Litzow MA, Abookire AA, Romano MD, Robards MD (2008) Distribution and spawning dynamics of capelin (*Mallotus villosus*) in Glacier Bay, Alaska: a cold water refugium. Fish Oceanogr 17:137–146

Aydin K, Gaichas S, Ortiz I, Kinzey D, Friday N (2007) A comparison of the Bering Sea, Gulf of Alaska, and Aleutian Islands large marine ecosystems through food web modeling. NOAA Tech Memo NMFS-AFSC-178. National Marine Fisheries Service, Seattle, WA

Blackburn JE, Jackson PB, Warner IM, Dick MH (1981) Survey for spawning forage fish on the east side of the Kodiak Archipelago by air and boat during spring and summer 1979. Final Report. National Ocean Service, Ocean Assessments Division, Anchorage, AK

Bond NA, Cronin MF, Freeland H, Mantua N (2015) Causes and impacts of the 2014 warm anomaly in the NE Pacific. Geophys Res Lett 42:3414–3420

Brown ED (2002) Life history, distribution, and size structure of Pacific capelin in Prince William Sound and the northern Gulf of Alaska. ICES J Mar Sci 59:983–996

Carscadden JE, Frank KT, Miller DS (1989) Capelin (*Mallotus villosus*) spawning on the southeast shoal: influence of physical factors past and present. Can J Fish Aquat Sci 46:1743–1754

Carscadden J, Nakashima BS, Frank KT (1997) Effects of fish length and temperature on the timing of peak spawning in capelin (*Mallotus villosus*). Can J Fish Aquat Sci 54:781–787

Cheng W, Hermann AJ, Coyle KO, Dobbins EL, Kachel NB, Stabeno PJ (2012) Macro- and micro-nutrient flux to a highly productive submarine bank in the Gulf of Alaska: a model-based analysis of daily and interannual variability. Prog Oceanogr 101:63–77

Cooper DW, Duffy-Anderson JT, Stockhausen WT, Cheng W (2013) Modeled connectivity between northern rock sole (*Lepidopsetta polyxystra*) spawning and nursery areas in the eastern Bering Sea. J Sea Res 84:2–12

Coyle KO, Pinchuk AI (2005) Seasonal cross-shelf distribution of major zooplankton taxa on the northern Gulf of Alaska shelf relative to water mass properties, species depth preferences and vertical migration behavior. Deep Sea Res II 52:217–245

Coyle KO, Gibson GA, Hedstrom K, Hermann AJ, Hopcroft RR (2013) Zooplankton biomass, advection and production on the northern Gulf of Alaska shelf from simulations and field observations. J Mar Syst 128:185–207

Coyle KO, Hermann AJ, Hopcroft RR (2019) Modeled spatial-temporal distribution of productivity, chlorophyll, iron and nitrate on the northern Gulf of Alaska shelf relative to field observations. Deep Sea Res II 165:163–191

Cury PM, Bakun A, Crawford RJM, Jarre A, Quiñones RA, Shannon LJ, Verheye HM (2000) Small pelagics in upwelling systems: patterns of interaction and structural changes in 'wasp-waist' ecosystems. ICES J Mar Sci 57: 603–618

Doyle MJ, Busby MS, Duffy-Anderson JT, Picquelle SJ, Matarese AC (2002) Early life history of capelin (*Mallotus villosus*) in the northwest Gulf of Alaska: a historical perspective based on larval collections, October 1977–March 1979. ICES J Mar Sci 59:997–1005

Doyle MJ, Strom SL, Coyle KO, Hermann AJ and others (2019) Early life history phenology among Gulf of Alaska fish species: strategies, synchronies, and sensitivities. Deep Sea Res II 165:41–73

Duffy-Anderson JT, Blood DM, Cheng W, Ciannelli L and others (2013) Combining field observations and modeling approaches to examine Greenland halibut (*Reinhardtius hippoglossoides*) early life ecology in the southeastern Bering Sea. J Sea Res 75:96–109

Etherington LL, Hooge PN, Hooge ER, Hill DF (2007) Oceanography of Glacier Bay, Alaska: implications for biological patterns in a glacial fjord estuary. Estuaries Coasts 30:927–944

Francis RC, Hare SR, Hollowed AB, Wooster WS (1998) Effects of interdecadal climate variability on the oceanic ecosystems of the NE Pacific. Fish Oceanogr 7:1–21

Francis RC, Hixon MA, Clarke ME, Murawski SA, Ralston S (2007) Ten commandments for ecosystem-based fisheries scientists. Fisheries 32:217–233

Frank KT, Leggett WC (1982) Environmental regulation of growth rate, efficiency, and swimming performance in larval capelin (*Mallotus villosus*), and its application to the match/mismatch hypothesis. Can J Fish Aquat Sci 39: 691–699

Gjøsæter H (1998) The population biology and exploitation of capelin (*Mallotus villosus*) in the Barents Sea. Sarsia 83:453–496

Goldstein ED, Duffy-Anderson JT, Matarese AC, Stockhausen WT (2019) Larval fish assemblages in the eastern and western Gulf of Alaska: patterns, drivers, and implications for connectivity. Deep Sea Res II 165:26–40

Haidvogel DB, Arango H, Budgell WP, Cornuelle BD and others (2008) Ocean forecasting in terrain-following coordinates: formulation and skill assessment of the Regional Ocean Modeling System. J Comput Phys 227: 3595–3624

Harper JR, Morris MC (2014) Alaska ShoreZone Coastal Habitat Mapping Protocol. Nuka Research and Planning, LCC for the Bureau of Ocean Energy Management (BOEM), Anchorage, AK

Hatch SA (2013) Kittiwake diets and chick production signal a 2008 regime shift in the Northeast Pacific. Mar Ecol Prog Ser 477:271–284

Hatch SA (2018) Middleton Island Seabird Research and Monitoring: 2018 Field Report. Institute for Seabird Research and Conservation, Anchorage, AK

Hermann AJ, Hinckley S, Dobbins EL, Haidvogel DB and others (2009) Quantifying cross-shelf and vertical nutrient flux in the Coastal Gulf of Alaska with a spatially nested, coupled biophysical model. Deep Sea Res II 56:2474–2486

Hollowed AB, Barange M, Beamish RJ, Brander K and others (2013) Projected impacts of climate change on marine fish and fisheries. ICES J Mar Sci 70:1023–1037

Jones DT, Lauffenberger N, Williams K, De Robertis A (2019) Results of the acoustic-trawl survey of walleye pollock (*Gadus chalcogrammus*) in the Gulf of Alaska, June-August 2017 (DY2017-06). AFSC Processed Rep 2019-08. Alaska Fisheries Science Center, NOAA, National Marine Fisheries Service, Seattle, WA

Kettle AB, Bargmann N, Winnard S (2015) Biological monitoring at East Amatuli Island, Alaska in 2014. AMNWR 2015/06. U.S. Fish and Wildlife Service, Alaska Maritime National Wildlife Refuge, Homer, AK

Ladd C, Stabeno P, Cokelet E (2005) A note on cross-shelf exchange in the northern Gulf of Alaska. Deep Sea Res II 52:667–679

Lanksbury J, Duffy-Anderson J, Mier K, Wilson M (2005) Ichthyoplankton abundance, distribution, and assemblage structure in the Gulf of Alaska during September 2000 and 2001. Estuar Coast Shelf Sci 64:775–785

Link JS (2002) What does ecosystem-based fisheries management mean? Fisheries 27:18–21

Lippiatt SM, Lohan MC, Bruland KW (2010) The distribution of reactive iron in northern Gulf of Alaska coastal waters. Mar Chem 121:187–199

Logerwell E, Busby M, Carothers C, Cotton S and others (2015) Fish communities across a spectrum of habitats in the western Beaufort Sea and Chukchi Sea. Prog Oceanogr 136:115–132

McGowan DW, Horne JK, Parker-Stetter SL (2019a) Variability in species composition and distribution of forage fish in the Gulf of Alaska. Deep Sea Res II 165:221–237

McGowan DW, Horne JK, Rogers LA (2019b) Effects of temperature on the distribution and density of capelin in the Gulf of Alaska. Mar Ecol Prog Ser 620:119–138

Mecklenburg CW, Steinke D (2015) Ichthyofaunal baselines in the Pacific Arctic region and RUSALCA study area. Oceanography 28:158–189

Mecklenburg CW, Lynghammar A, Johansen E, Byrkjedal I and others (2018) Marine fishes of the Arctic region Vol 1. Conservation of Arctic Flora and Fauna, Akureyri

Merrick RL, Chumbley MK, Byrd GV (1997) Diet diversity of Steller sea lions (*Eumetopias jubatus*) and their population decline in Alaska: a potential relationship. Can J Fish Aquat Sci 54:1342–1348

Mordy CW, Stabeno PJ, Kachel NB, Kachel D and others (2019) Patterns of flow in the canyons of the northern Gulf of Alaska. Deep Sea Res II 165:203–220

Mueter F, Norcross B (2002) Spatial and temporal patterns in the demersal fish community on the shelf and upper slope regions of the Gulf of Alaska. Fish Bull 100: 559–581

Mundy PR (2005) The Gulf of Alaska: biology and oceanog-

raphy. University of Alaska Fairbanks, Alaska Sea Grant College Program, Fairbanks, AK

Nakashima BS, Taggart CT (2002) Is beach-spawning success for capelin, *Mallotus villosus* (Müller), a function of the beach? ICES J Mar Sci 59:897–908

Naumenko EA (1996) Distribution, biological condition, and abundance of capelin (*Mallotus villosus socialis*) in the Bering Sea. In: Mathisen OA, Coyle KO (eds) Ecology of the Bering Sea: a review of Russian literature. Report 96–01. University of Alaska Sea Grant College Program, Fairbanks, AK, p 306

O'Driscoll RL, Rose GA, Anderson JT (2002) Counting capelin: a comparison of acoustic density and trawl catchability. ICES J Mar Sci 59:1062–1071

Oliver ECJ, Donat MG, Burrows MT, Moore PJ and others (2018) Longer and more frequent marine heatwaves over the past century. Nat Commun 9:1324

Pahlke KA (1985) Preliminary studies of capelin (*Mallotus villosus*) in Alaskan waters. Alaska Department of Fish and Game, Juneau, AK

Parker-Stetter SL, Horne JK, Farley EV, Barbee DH, Andrews AG III, Eisner LB, Nomura JM (2013) Summer distributions of forage fish in the eastern Bering Sea. Deep Sea Res II 94:211–230

Piatt JF, Anderson PJ (1996) Response of common murres to the *Exxon Valdez* oil spill and long-term changes in the Gulf of Alaska marine ecosystem. Am Fish Soc Symp 18: 720–737

Piatt JF, Arimitsu ML, Sydeman WJ, Thompson SA and others (2018) Biogeography of pelagic food webs in the North Pacific. Fish Oceanogr 27:366–380

Pikitch EK, Santora C, Babcock EA, Bakun A and others (2004) Ecosystem-based fishery management. Science 305:346–347

Royer T (1982) Coastal fresh-water discharge in the northeast Pacific. J Geophys Res 87:2017–2021

Sætre R, Gjøsæter J (1975) Ecological investigations on the spawning grounds of the Barents Sea capelin. Fiskeridir Skr Ser Havunders 16:203–227

Shchepetkin AF, McWilliams JC (2005) The regional oceanic modeling system (ROMS): a split-explicit, free-surface, topography-following-coordinate oceanic model. Ocean Model 9:347–404

Sohn D (2016) Distribution, abundance, and settlement of slope-spawning flatfish during early life stages in the Eastern Bering Sea. PhD dissertation, Oregon State University, Corvallis, OR

Speckman SG, Piatt JF, Minte-Vera CV, Parrish JK (2005) Parallel structure among environmental gradients and three trophic levels in a subarctic estuary. Prog Oceanogr 66:25–65

Stabeno PJ, Bond NA, Hermann AJ, Kachel NB, Mordy CW, Overland JE (2004) Meteorology and oceanography of the Northern Gulf of Alaska. Cont Shelf Res 24: 859–897

Stabeno PJ, Bell S, Cheng W, Danielson S, Kachel, NB, Mordy CW (2016a) Long-term observations of Alaska Coastal Current in the northern Gulf of Alaska. Deep Sea Res II 132:24–40

Stabeno PJ, Bond NA, Kachel NB, Ladd C, Mordy CW, Strom SL (2016b) Southeast Alaskan shelf from southern tip of Baranof Island to Kayak Island: currents, mixing and chlorophyll-*a*. Deep Sea Res II 132:6–23

Stergiou KI (1989) Capelin *Mallotus villosus* (Pisces: Osmeridae), glaciations, and speciation: a nomothetic approach to fisheries ecology and reproductive biology. Mar Ecol Prog Ser 56:211–224

Stockhausen WT, Coyle KO, Hermann AJ, Doyle M and others (2019) Running the gauntlet: connectivity between natal and nursery areas for Pacific ocean perch (*Sebastes alutus*) in the Gulf of Alaska, as inferred from a biophysical individual-based model. Deep Sea Res II 165:74–88

Strom SL, Olson MB, Macri EL, Mordy CW (2006) Cross-shelf gradients in phytoplankton community structure, nutrient utilization, and growth rate in the coastal Gulf of Alaska. Mar Ecol Prog Ser 328:75–92

Sydeman WJ, Piatt JF, Thompson SA, García-Reyes M and others (2017) Puffins reveal contrasting relationships between forage fish and ocean climate in the North Pacific. Fish Oceanogr 26:379–395

Waite JN, Mueter FJ (2013) Spatial and temporal variability of chlorophyll-*a* concentrations in the coastal Gulf of Alaska, 1998–2011, using cloud-free reconstructions of SeaWiFS and MODIS-Aqua data. Prog Oceanogr 116: 179–192

Wilson M, Brown A, Mier K (2005) Geographic variation among age-0 walleye pollock (*Theragra chalcogramma*): evidence of mesoscale variation in nursery quality? Fish Bull 103:207–218

Wilson MT, Jump CM, Duffy-Anderson JT (2006) Comparative analysis of the feeding ecology of two pelagic forage fishes: capelin *Mallotus villosus* and walleye pollock *Theragra chalcogramma*. Mar Ecol Prog Ser 317:245–258

Wilson MT, Mier KL, Jump CM (2013) Effect of region on the food-related benefits to age-0 walleye pollock (*Theragra chalcogramma*) in association with midwater habitat characteristics in the Gulf of Alaska. ICES J Mar Sci 70:1396–1407

Witteveen BH, Foy RJ, Wynne KM, Tremblay Y (2008) Investigation of foraging habits and prey selection by humpback whales (*Megaptera novaeangliae*) using acoustic tags and concurrent fish surveys. Mar Mamm Sci 24:516–534

Wolter K, Timlin MS (1993) Monitoring ENSO in COADS with a seasonally adjusted principal component index. In: Proc 17th Climate Diagnostics Workshop. NOAA/NMC/CAC, NSSL, Oklahoma Climate Survey, CIMMS and the School of Meteorology, University of Oklahoma, Norman, OK, p 52–57

Wolter K, Timlin MS (1998) Measuring the strength of ENSO events: How does 1997/98 rank? Weather 53:315–324

Zador S, Yasumishii EC (2017) Ecosystem considerations 2017: status of the Gulf of Alaska marine ecosystem. North Pacific Fishery Management Council, Anchorage, AK

Zimmermann M, Prescott MM (2015) Smooth sheet bathymetry of the central Gulf of Alaska. NOAA Tech Memo NMFS-AFSC-287. National Marine Fisheries Service, Seattle, WA

Editorial responsibility: Alejandro Gallego, Aberdeen, UK

Submitted: August 25, 2019; Accepted: December 2, 2019
Proofs received from author(s): February 24, 2020